อนุพันธ์ไคโทซานที่ตอบสนองต่ออุณหภูมิสำหรับการปลดปล่อยกลิ่นหอมแบบควบคุม

นางสาวจิราพร สีหมอก

วิทยานิพนธ์นี้ เป็นส่วนหนึ่งของการศึกษาตามหลักสูตรปริญญาวิทยาศาสตรมหาบัณฑิต
สาขาวิชาปิโตรเคมีและวิทยาศาสตร์พอลิเมอร์
คณะวิทยาศาสตร์ จุฬาลงกรณ์มหาวิทยาลัย
ปีการศึกษา 2554

THERMORESPONSIVE CHITOSAN DERIVATIVE FOR CONTROLLED RELEASE OF FRAGRANCES

Miss Jiraporn Seemork

A Thesis Submitted in Partial Fulfillment of the Requirements
for the Degree of Master of Science Program in Petrochemistry and Polymer Science
Faculty of Science
Chulalongkorn University
Academic Year 2011

Thesis Title	THERMORESPONSIVE CHITOSAN DERIVATIVE FOR CONTROLLED RELEASE OF FRAGRANCES
By	Miss Jiraporn Seemork
Field of Study	Petrochemistry and Polymer Science
Thesis Advisor	Associate Professor Supason Wanichwecharungruang, Ph.D.

Accepted by the Faculty of Science, Chulalongkorn University in Partial Fulfillment of the Requirements for the Master's Degree

……Dean of the Faculty of Science
(Professor Supot Hannongbua, Dr.rer.nat.)

THESIS COMMITTEE

……Chairman
(Assistant Professor Warinthorn Chavasiri, Ph.D.)

……Thesis Advisor
(Associate Professor Supason Wanichwecharungruang, Ph.D.)

……Examiner
(Associate Professor Voravee Hoven, Ph.D.)

……External Examiner
(Thitinun Karpkird, Ph.D.)

จิราพร สีหมอก : อนุพันธ์ไคโทซานที่ตอบสนองต่ออุณหภูมิสำหรับการปลดปล่อยกลิ่นหอมแบบควบคุม. (THERMORESPONSIVE CHITOSAN DERIVATIVE FOR CONTROLLED RELEASE OF FRAGRANCES) อ. ที่ปรึกษาวิทยานิพนธ์หลัก: รศ.ดร.ศุภศร วนิชเวชารุ่งเรือง, 65 หน้า.

โคพอลิเมอร์ของไคโตซานที่มีทั้งส่วนที่ชอบน้ำและไม่ชอบน้ำได้ถูกสังเคราะห์ขึ้นเพื่อใช้เป็นระบบปลดปล่อยกลิ่นแบบควบคุม พอลิเมอร์ที่สังเคราะห์ขึ้นมานี้สามารถเกิดการรวมตัวกันเองได้ในสารละลายที่มีน้ำเป็นตัวทำละลายและเกิดเป็นอนุภาคทรงกลมในงานวิจัยนี้ พอลิเอทิลีนไกลคอลซึ่งเป็นพอลิเมอร์ที่ชอบน้ำถูกติดลงบนไคโตซานเพื่อเป็นส่วนที่ทำหน้าที่เป็นพอลิเมอร์ที่ตอบสนองต่ออุณหภูมิและเป็นส่วนเปลือกนอกของอนุภาค ในขณะที่แอลดีไฮด์ที่ให้กลิ่น ซึ่งในงานวิจัยนี้ ใช้ วานิลลิน และซิทรอลถูกติดลงไปบนไคโตซานเพื่อทำหน้าที่เป็นส่วนที่ไม่ชอบน้ำ และเป็นส่วนแกนของอนุภาค อนุภาคพอลิเมอร์ที่สังเคราะห์ได้แสดงสมบัติการเกาะกลุ่มและการแยกออกจากกันที่ขึ้นกับอุณหภูมิซึ่งนำไปสู่การปลดปล่อยกลิ่นที่สามารถควบคุมได้ด้วยอุณหภูมิ แอลดีไฮด์จะถูกปลดปล่อยอย่างมีนัยสำคัญจากอนุภาคที่อุณหภูมิต่ำกว่าอุณหภูมิการละลายวิกฤติตอนล่าง แต่การปลดปล่อยจะช้าลงอย่างชัดเจนเมื่ออุณหภูมิสูงขึ้นเกินกว่าอุณหภูมิการละลายวิกฤติตอนล่าง นอกจากนั้นอุณหภูมิการละลายวิกฤติตอนล่างยังสามารถถูกปรับได้โดยการเปลี่ยนความเข้มข้นของเกลือ และมากไปกว่านั้นระบบการปลดปล่อยแบบควบคุมนี้ เป็นระบบที่สามารถเข้ากันได้ดีกับสิ่งมีชีวิต จึงมีความปลอดภัยกว่าและสามารถประยุกต์ใช้ประโยชน์ได้หลากหลายด้าน

สาขาวิชา ปิโตรเคมีและวิทยาศาสตร์พอลิเมอร์ ลายมือชื่อนิสิต .....

ปีการศึกษา 2554 ลายมือชื่อ อ.ที่ปรึกษาวิทยานิพนธ์หลัก .....

5272254523: MAJOR PETROCHEMISTRY AND POLYMER SCIENCE
KEYWORDS: THERMOREPONSIVE CHITOSAN/ CONTROLLED RELEASE/ PERFUMERY ALDEHYDE

JIRAPORN SEEMORK: THERMORESPONSIVE CHITOSAN DERIVATIVE FOR CONTROLLED RELEASE OF FRAGRANCES. ADVISOR: ASSOC. PROF. SUPASON WANICHWECHARUNGRUANG, Ph.D., 65 pp.

The amphiphilic thermoresponsive chitosan derivative was synthesized for using as a fragrance controlled release system. The obtained polymer could self-assemble in aqueous media to form polymeric particles with spherical shape. Poly(ethylene glycol), a hydrophilic polymer, was grafted onto chitosan backbone in order to act as thermoresponsive residue in which upon self-assembling became particles' coronas, whereas perfumery aldehyde (in this case vanillin and citral) was grafted onto the chitosan to inherit hydrophobicity which upon self-assembling became particles' core. The synthesized thermoresponsive polymer showed aggregation-dissociation behavior, corresponding with temperature trigger, leading to temperature dependence of the fragrance controlled release; significantly release of aldehyde from the particles was observed when the temperature was lower than lower critical solution temperature (LCST) whereas slower release was obvious at the temperature beyond the LCST. The LCST of system could be tuned by adjusting through salt concentration. This delivery system is completely biocompatible, therefore, it can be used in various applications.

Field of Study: Petrochemistry and Polymer Science Student's Signature .....

Academic Year 2011 Advisor's Signature .....

ACKNOWLEDGEMENTS

Firstly, I would like to express my sincere thankfulness to my thesis advisor, Associate Professor Dr. Supason Wanichwecharungruang for her helpful suggestion and encouragement to accomplish my thesis.

Furthermore, I gratefully thank Assistant Professor Dr. Warinthorn Chavasiri, Associate Professor Dr. Voravee Hoven and Dr. Thitinun Karpkird for their valuable advices and comments as the committee members.

I also would like to thank National Center of Excellence for Petrochemicals and Advanced Materials (NCE-PPAM) and the Graduate School, Chulalongkorn University for financial support. Moreover, I gratefully thank Professor Masayuki Yamaguchi and Dr. Murakami Tatsuya, School of Materials Science, Japan Advanced Institute of Science and Technology for XPS analysis, Associate Professor Dr. Sanong Ekgasit for ATR-FTIR characterization and Associate Professor Dr. Tirayut Vilaivan, Organic Synthesis Research Unit (OSRU), Chulalongkorn University for the free access of temperature control UV-Visible spectrophotometer.

Finally, I would like to specially thank my family and friends, especially in my laboratory for their understanding, helpfulness and suggestion throughout my master study.

CONTENTS

Page

LIST OF TABLES

LIST OF FIGURES

Figure **Page**

Figure **Page**

Figure **Page**

LIST OF SCHEMES

LIST OF ABBREVIATIONS

ATR-FTIR	attenuated total reflectance fourier transform infrared
δ	chemical shift
°C	degree Celsius
Da	degree of deacetylation
DG	degree of grafting
g	gram (s)
Hz	hertz
kV	kilovolt (s)
µl	microliter (s)
µm	micrometer (s)
mA	milliampere
mg	milligram (s)
mL	milliliter (s)
mm	millimeter (s)
min	minute (s)
MW	molecular weight
nm	nanometer
NMR	nuclear magnetic resonance
ppm	parts per million
%	prcent
SPM	scanning probe microscope
TEM	transmission electron microscope
UV	ultraviolet
cm^{-1}	unit of wavenumber (IR)
λ	wavelength
XPS	X-ray Photoelectron Spectroscopy

CHAPTER I
INTRODUCTION

Fragrance has been used for enhancement of pleasant odor in daily life products such as shampoos, soaps, deodorants, detergents and cosmetics. Fragrant chemical can be categorized in accordance with their chemical functionality, e.g., alcohols, aldehydes, ketones, esters, lactones, ethers and nitriles [1].

Among the various kinds of fragrance, aldehydes are the popularly used one owing to the variety of their odors. However, due to their volatility and reactivity, they are, therefore, easy to evaporate, leading to instability, low efficiency and short-time usage. These problems take place not only for aldehydes but also other fragrant chemicals. To overcome these drawbacks, various fragrance controlled release technologies have been fabricated in order to prolong the longevity and increase not only the stability but also efficiency [2]. In general, there are two strategies of the fragrance controlled release technology; one is physical encapsulation of which fragrant molecules were trapped inside well-designed polymer matrix in order to control their evaporation and protect their degradation from the environmental stimuli such as temperature, moisture, pH, chemical reaction, light and enzyme. While, the other one is chemical derivation, fragrant molecules are formed covalent bonds with appropriate moieties to obtained precursor species, pro-fragrances such as β-mercapto ketones [3], β -amino-alcohol [4] and acetal [5], which are labile under specific conditions and can reversibly be original fragrant molecules with cleavage of the chemical bonds by the trigger. There are various kinds of the trigger or environment stimuli for cleavage of covalent bonds as follows:

Temperature

The first fragrance controlled release technology which has been fabricated was the heat-activated delivery system. Heating is the most common method to break several types of chemical bond. Heating is considered as a general condition in everyday life such as release of some flavor additives from food during cooking. The

sample of heat-activated precursor shown in the Figure 1.1 is derivative of aldehydes and cyclic acetals.

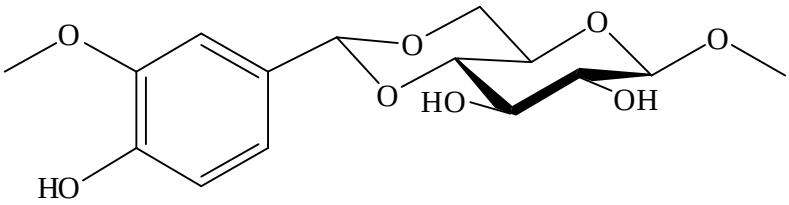

Figure 1.1 Heat-activated precursor of aldehyde derivative [1]

Oxidation

Oxygen species is well-known as one of the most reactive species which can react with several functional groups through oxidation reaction. Oxidative degradation of the labile functional groups seems to be easy to occur because an abundance of reactive oxygen species in the environment. However, it is quite difficult to control the oxidation reaction, herefore, there are little literatures involving the release of pro-fragrances by oxygen stimulus.

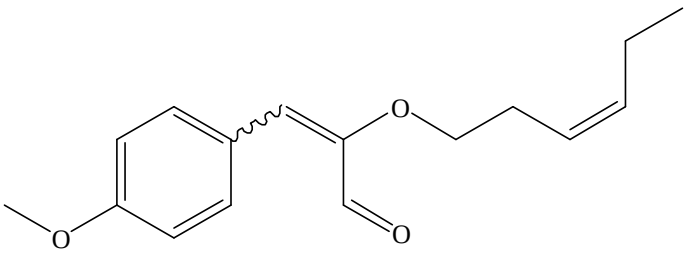

Figure 1.2 Oxidative bond cleavage precursor of aldehyde derivative [1]

Light

As well known, light, especially sunlight, is the most important energy source for living organisms. The light of which wavelength is close to UV region possesses ability to cleavage covalent bonds. For example, Norrish type II photofragmentation of carbonyl derivatives which yields a carbonyl and alkene compound. Alkyl phenyl ketone derivatives are the most general precursor which can undergo the Norrish type II photoreaction.

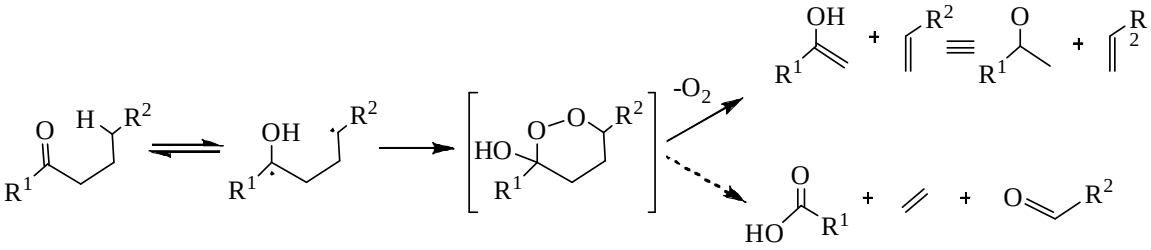

Figure 1.3 Mechanism of Norrish type II photofragmentation [1]

Hydrolysis and change of the pH value

The most used medium in perfumery applications and hydrolysis is water. It may be a suitable trigger for controlled release of fragrances by change of pH value. Most release or chemical delivery systems of volatiles described in literatures, is based on hydrolysis bond cleavage of various types of precursor.

Chitosan

Chitosan, a chitin derivative which is composed of β-(1-4)-2-amino-2-deoxy-D-glucopyranose residues and β-(1-4)-2-acetamido-2-deoxy-D-glucopyranose units, is widely used in various applications such as pharmaceuticals, cosmetics, foods and agricultures because of its biodegradability, biocompatibility and non-toxicity, leading to advanced developments i.e. chemical modifications.

Poly(ethylene oxide) modified chitosan

In 2005, Hu et al synthesized poly(ethylene glycol)-*g*-chitosan (PEG-*g*-CS) using reaction between methoxy poly(ethylene glycol) iodide (MPEG-I) and triphenylmethyl chitosan (TPM-CS) in organic solvent.

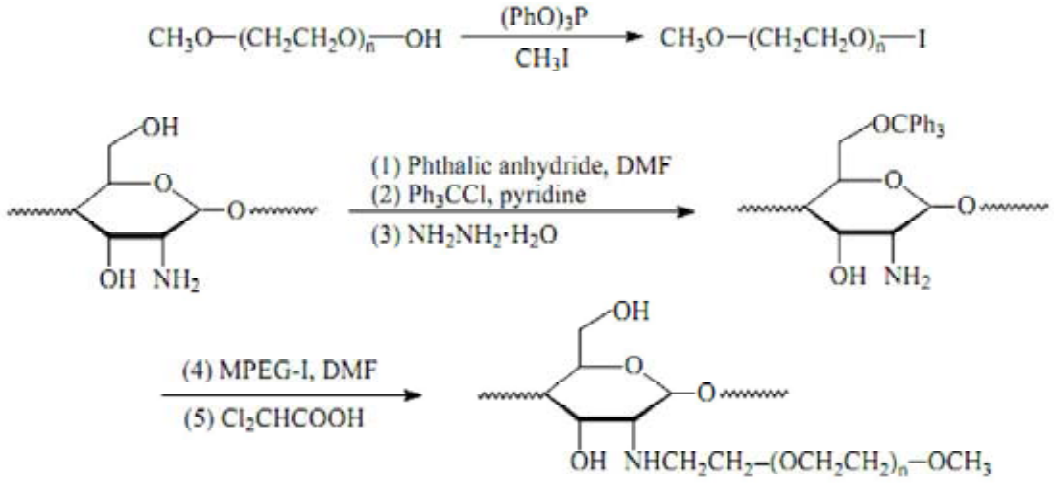

Figure 1.4 Schematic illustration of synthesis of PEG-*g*-CS [6]

The result indicates that use of organosoluble 6-O-triphenylmethylchitosan as a precursor and then reacted with PEG iodide in homogeneous reaction using polar organic medium, allowed the nucleophilic substitution reactions to conduct, resulting in high DS and well-controlled reaction. Moreovere, it has been found that the copolymers was soluble in water in wide range of pH value.

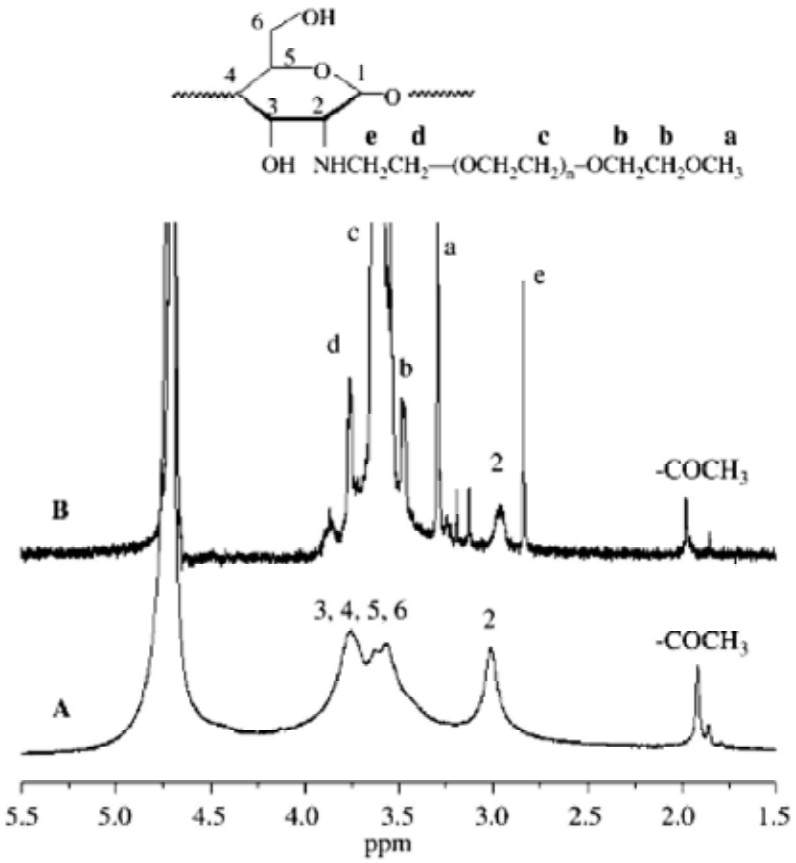

Figure 1.5 ^{1}H NMR spectra of (A) chitosan in 1% (v/v) CD_3COOD/D_2O and (B) PEG-*g*-chitosan in D_2O [6]

In 2006, Fangkangwanwong et al synthesized chitosan which was modified with poly(ethylene glycol) methyl ether (mPEG) at the amino and hydroxyl groups. The product was obtained from a one-pot homogeneous reaction in aqueous media.

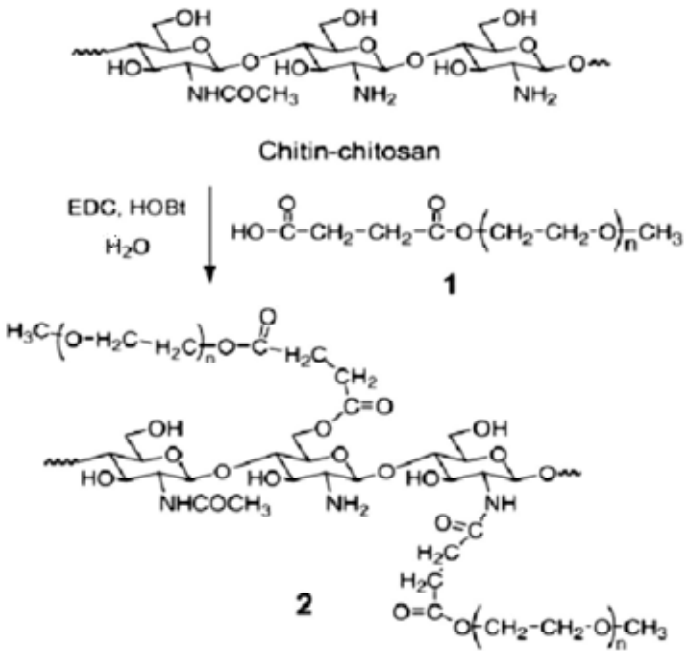

Figure 1.6 Schematic illustration of preparation of chitosan-*g*-mPEG in an aqueous media [7]

^{1}H NMR spectrum shows that mPEG was successfully grafted on chitosan via heterogeneous coupling reaction in aqueous media. The chitosan-g-mPEG with 24 %DS was soluble in water and swellable in methanol and chloroform.

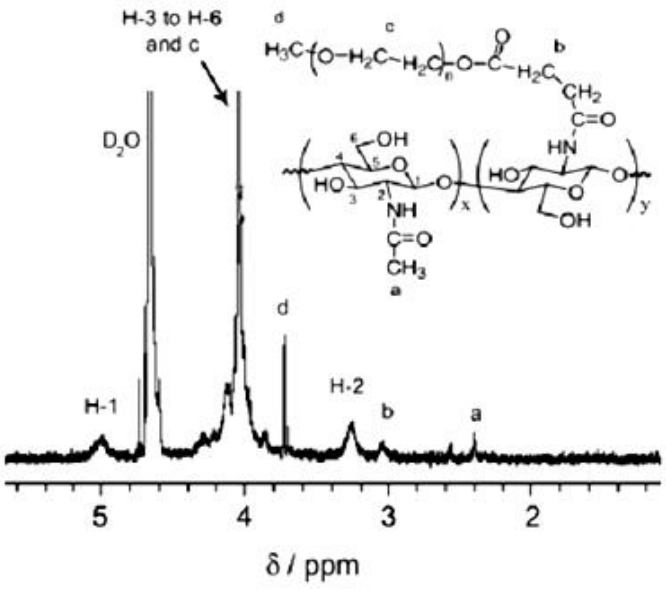

Figure 1.7 ^{1}H NMR spectrum of chitosan-*g*-mPEG in D_2O at 70 ^{o}C [7]

In 2008, Yoksan et al synthesized amphiphilic chitosan by grafting chitosan with hydrophobic residues, phathaloyl groups, and poly(ethylene glycol), a hydrophilic moiety, to obtain a well-dispersed solution in polar solvents and, moreover, achieve a nanoparticle (~ 200 nm) which possessed negative charge at the surface.

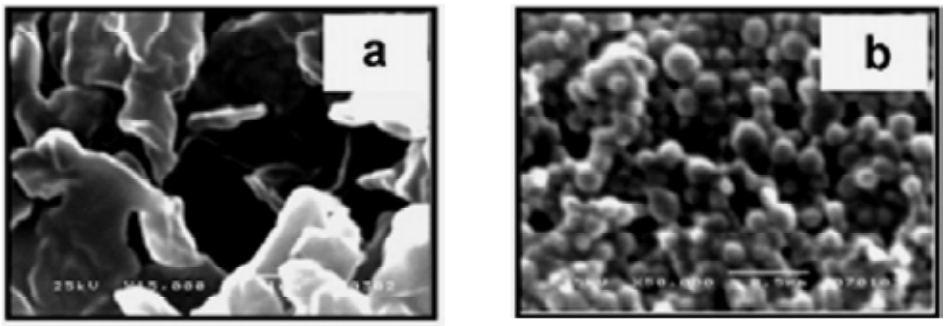

Figure 1.8 SEM photographs of (a) chitosan (15,000x) and (b) *N*-phthaloylchitosan grafted mPEG (50,000x) [8]

Thermoresposive polymers

Thermoresponsive polymer is a polymer of which physical properties response to temperature stimulus. When the temperature is below the critical solution temperature (LCST), the polymer could be miscible in a medial but when the temperature is raised up beyond the LCST, the polymer would be insoluble. Thermoresponsive polymers have attracted much research interest because of their potential applications such as rheological control additives, controlled release of drugs and gene therapy [9].

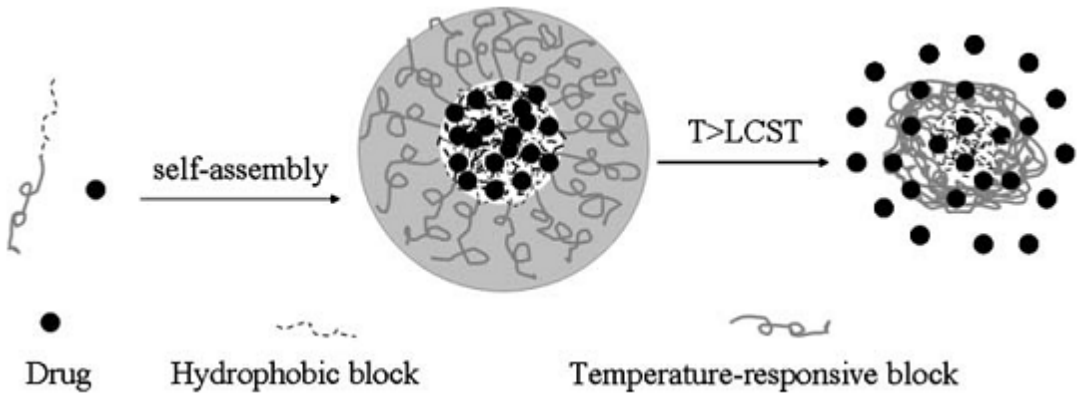

Figure 1.9 Schematic illustration of thermoresponsive polymer used as drug delivery system [9]

In 2009, Morinaga et al synthesized a new amphiphilic copolymers of polymethacrylate grafting with a lilial-derived acetal which behaved like a hydrophobic part and PEG which possessed a hydrophilic character. The copolymers could self-assemble in aqueous media to form polymeric micelles, of which aggregation-dissociation responded sharply and reversibly on temperature in the presence of NaCl. The copolymers, moreover, show efficiency for a temperature-switchable control release of perfumery aldehyde, lilial, which was grafted on the polymer backbone.

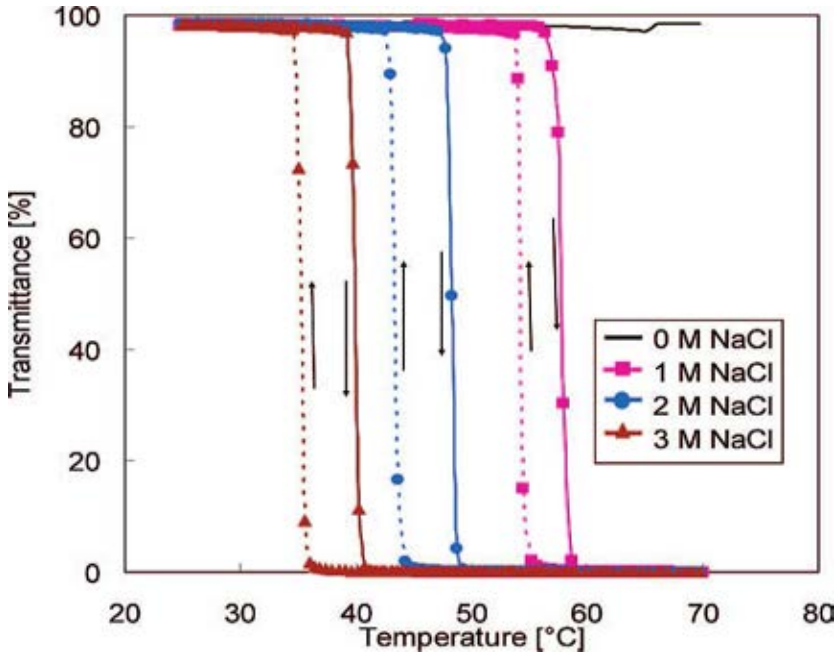

Figure 1.10 Temperature dependence of thermoresponsive copolymers in aqueous media with various concentrations of NaCl: solid line: 25 to 70 °C; broken line: 70 to 25 °C. [5]

As seen in the figure, the release of lilial from the thermoresponsive copolymers in the presence of NaCl and pH 3.0 at the temperature above LCST was minimal while the release at the temperature below the LCST was obviously faster.

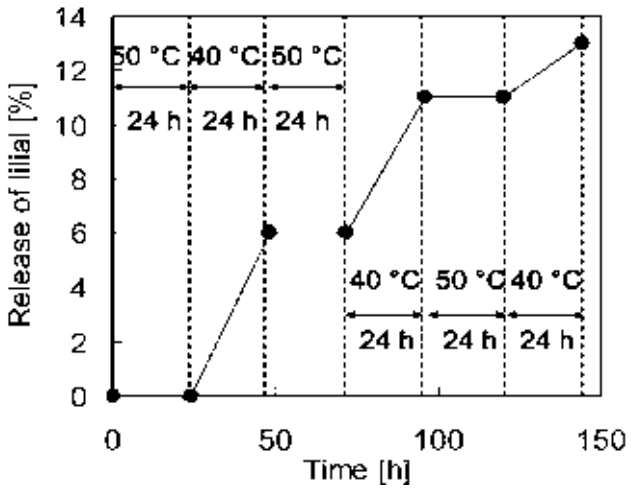

Figure 1.11 Controlled release of lilial from the thermoresponsive copolymers in buffer solution (pH = 3.0) with the presence of NaCl (2.0 M) at 40 and 50 ^{o}C [5]

In 2011, Hua et al reported a green chemistry method to synthesize chitosan grafted with hydrophobic residues, lilial, via Schiff base bond formation. Then the thermoresponsive polymer, *N*-isopropylacrylamide was grafted to the lilial-modified chitosan to obtain an amphiphilic copolymers. The obtained amphihilic copolymers could self-assemble in water at neutral pH into nanoparticles with the spherical size for 142±60 nm [10].

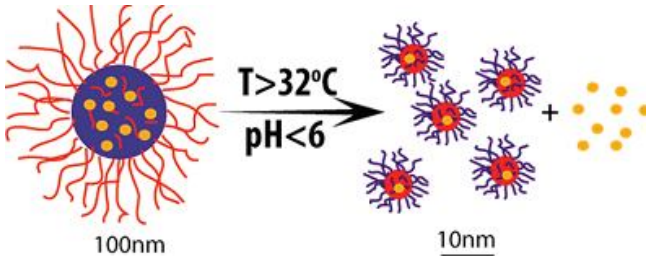

Figure 1.12 Schematic illustration of the temperature and pH responsive behavior of self-assembled PNIPAm-CS-Lilial nanoparticles. PNIPAm, CS and lilial are represented in red, blue and yellow, respectively. [10]

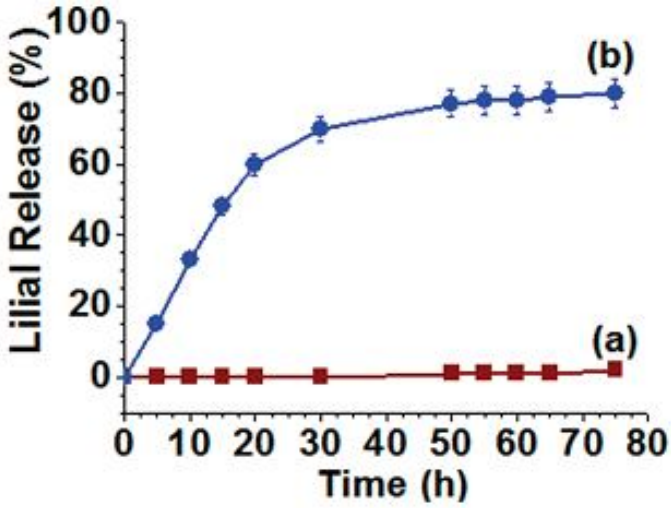

Figure 1.13 Lilial release profile at (a) 25 ^{o}C, pH = 7.4 and (b) 37 ^{o}C, pH = 4.5 [10]

Chitosan Shiff base derivatives

In 2005, dos Santos et al prepared Schiff base from chitosan and salicylaldehyde derivatives and found that the substitution degrees depended on the R group of salicylaldehyde, varying from 4.6 to 68.5%.

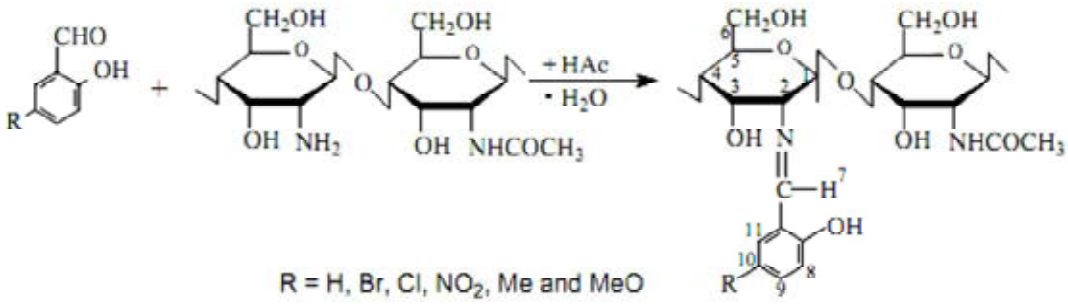

Figure 1.14 Schematic illustration of reaction of the chitosan modified with substituted salicylaldehydes, where R=H, Br, Cl, NO_2, Me, MeO [11].

In 2006, Guinesi et al investigated the effect of some reaction parameters, mol ratio (salicylaldehyde:free amino groups), reaction time and temperature. It has been

found that the reaction parameters had influenced to the substitution degree (DS) in the preparation of Schiff bases from chitosan.

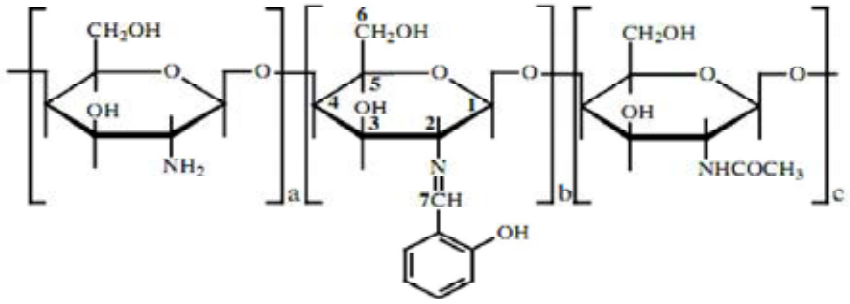

Figure 1.15 Schematic representation of chitosan Schiff base chemical structure [12]

The IR spectra of the chitosan Shiff bases show a strong absorption peak at 1631.6 cm^{-1} corresponded to the C=N vibrations of imines bond. In addition, there is no absorption peak attributed to the free aromatic aldehydes.

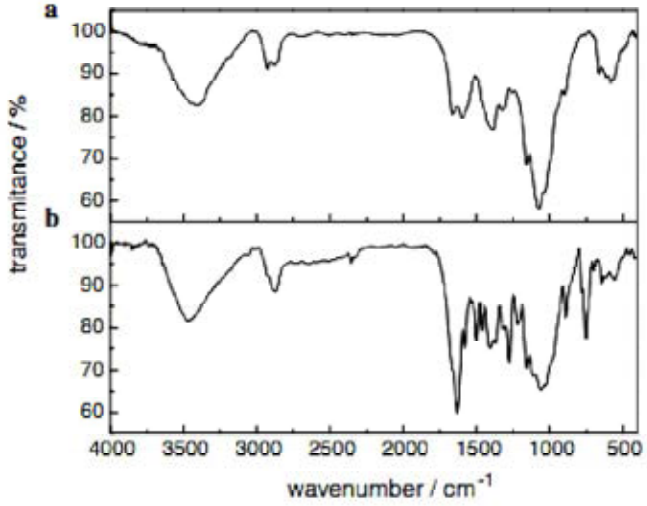

Figure 1.16 FTIR spectra of (a) chitosan and (b) chitosan Schiff base (%DS = 21.9%) [12]

In 2008, Jin et al synthesized the Schiff base of chitosan using the reaction between chitosan and citral under high-intensity ultrasound. The products showed antimicrobial activities against *Escherichia coli*, *Staphylococcus aureus*, and *Aspergillus niger*. FTIR spectroscopy was used to characterize the structure of the Schiff base. The strong peaks at 1648.3 and 1610.6 cm^{-1}, attributed to C=N and C=C stretching vibrations, could be observed. These results indicated that amino groups of chitosan could be reacted with citral to form the Schiff base.

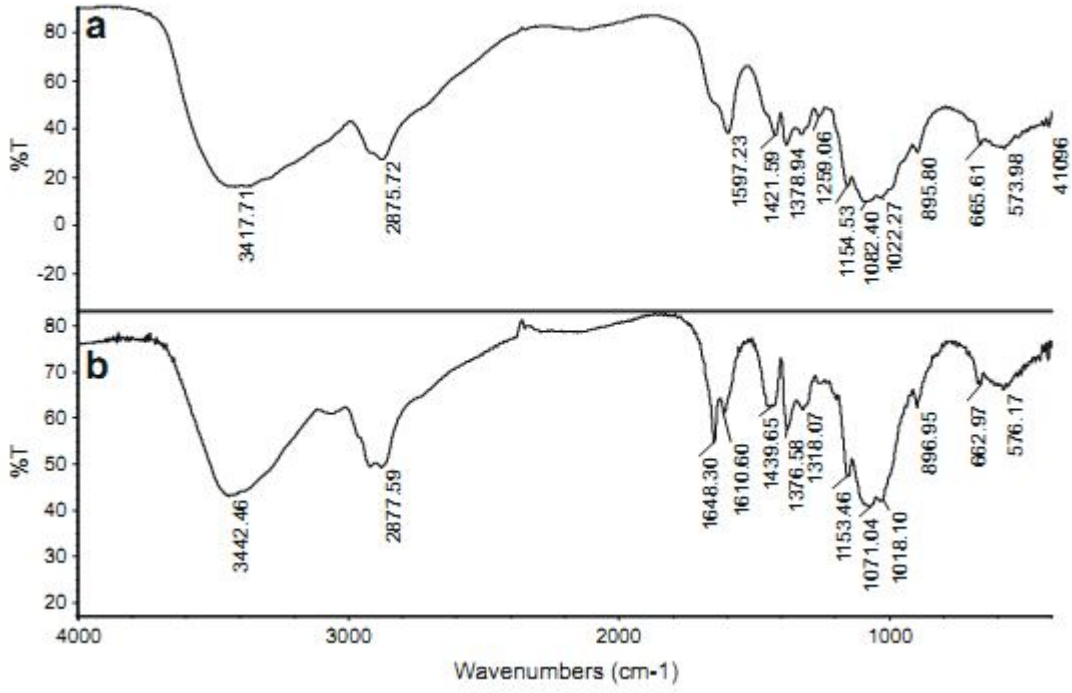

Figure 1.17 FTIR spectra of (a) chitosan and (b) chitosan Schiff base [13]

In 2011, Tree-udom et al synthesized double barriers carrier for controlled release of fragrances using *N*-succinylchitosan (*N*-SCS), a modified polymer which could well disperse in water and self-assemble into polymeric nanoparticles with a spherical shape (hydrodynamic diameter size was 46.3 ± 0.24 nm and PDI was 0.1850). Then, the fragrant molecules, perfumery aldehydes, were grafted on *N*-succinylchitosan *via* Schiff base formation in aqueous media under high-intensity ultrasonication.

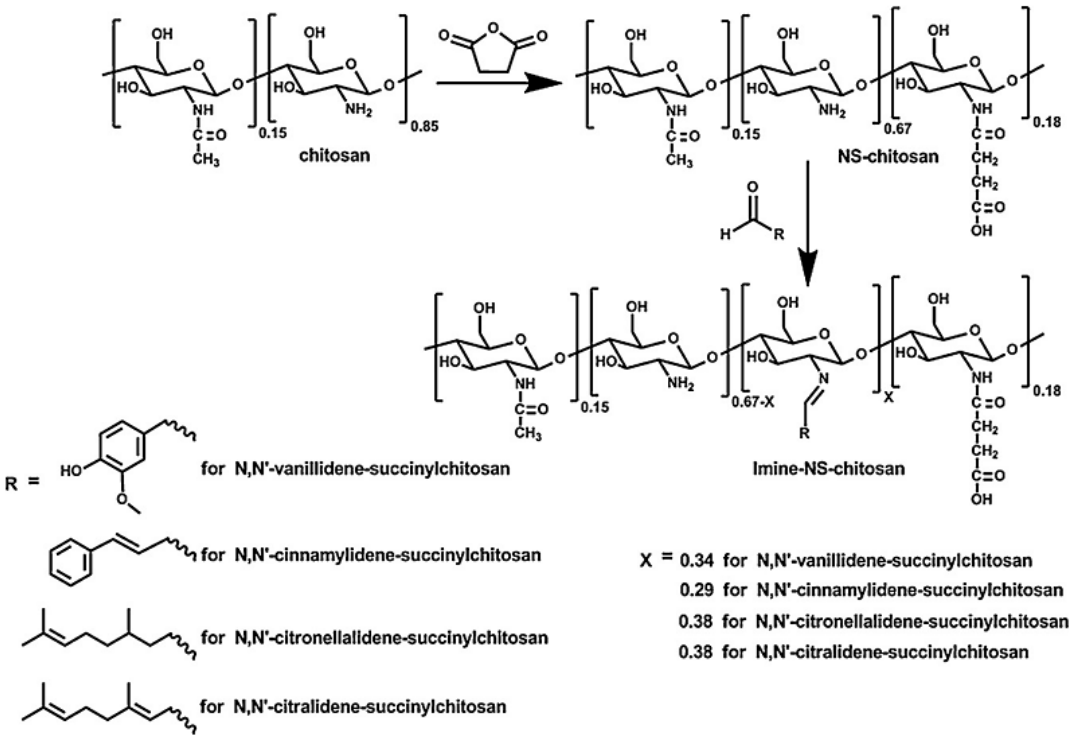

Figure 1.18 Schematic representation of synthesis of *N,N'*-imine-succinylchitosan [14]

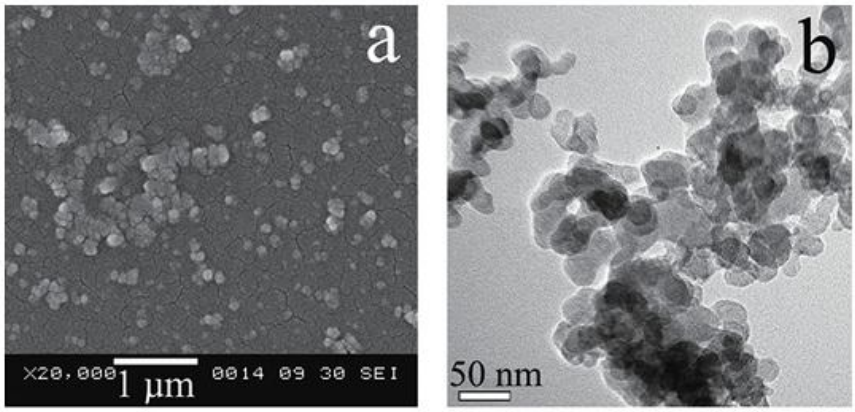

Figure 1.19 (a) SEM and (b) TEM photographs of *N*-succinylchitosan [14]

XPS high resolution spectra of the products were used to confirm that the perfumery aldehydes were successfully grafted on *N*-succinylchitosan and the grafted aldehydes, moreover, were embeded at particles' core and behaved as a hydrophobic residue when the nanoparticles self-assembled in the aqueous.

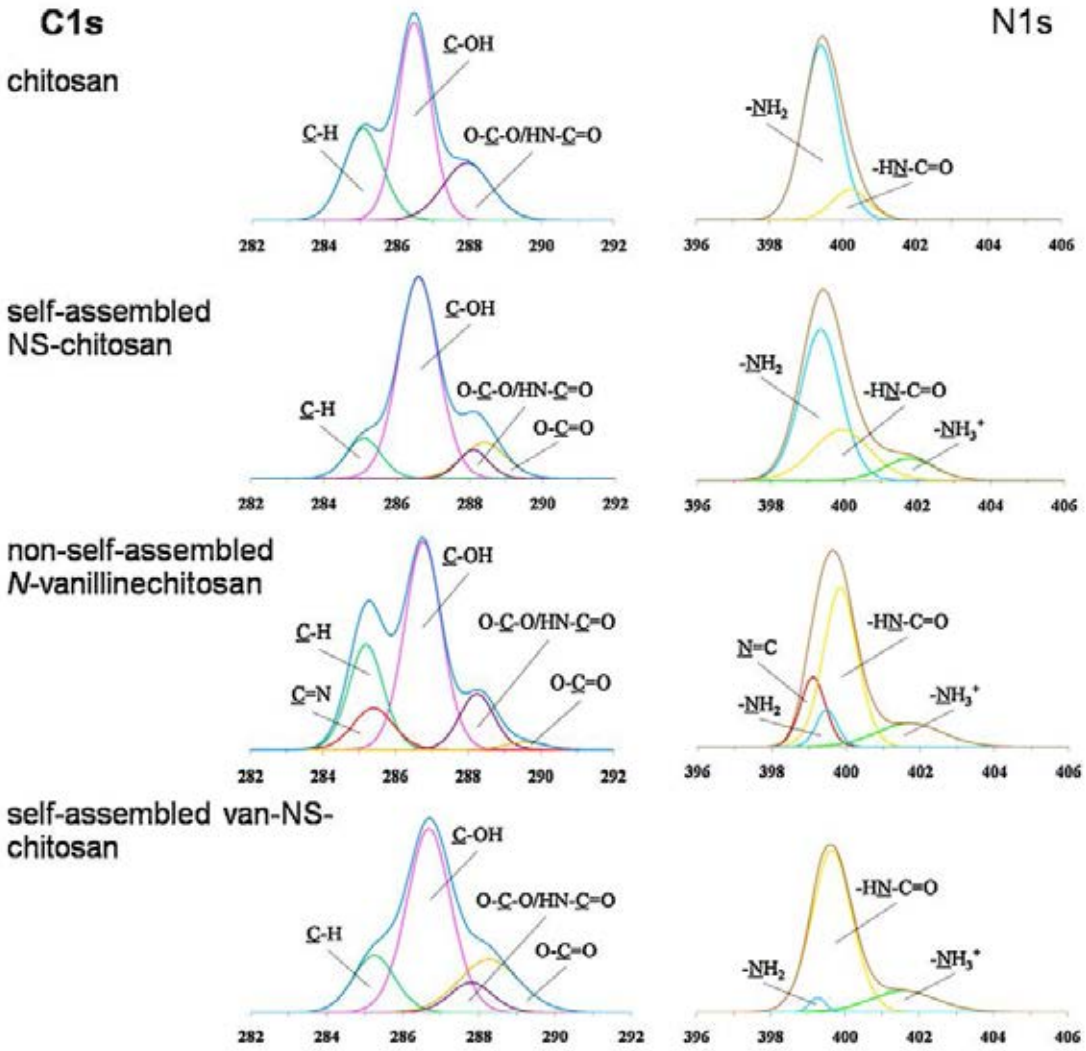

Figure 1.20 XPS spectra of the various products [14]

Furthermore, the fragrant nanocarriers showed controlled release of the grafted aldehydes when compared with free aldehydes. The release of perfumery aldehydes from the double barriers carrier was obviously slower than that of free aldehydes.

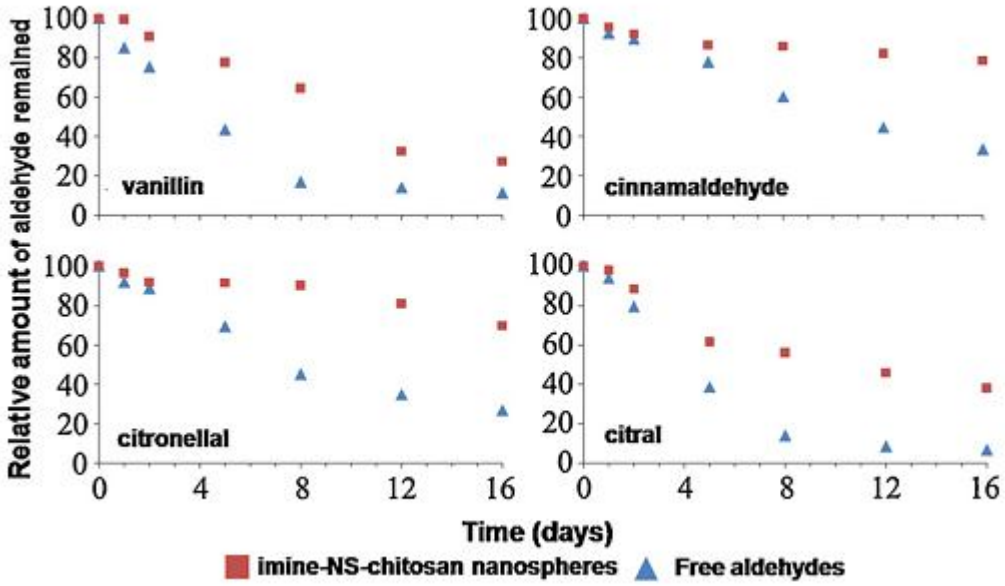

Figure 1.21 Release profiles of aldehydes from *N,N'*-imime-succinylchitosan nanocarriers compared with free aldehydes [14]

Perfumery aldehydes

Vanillin

Vanillin, 4-Hydroxy-3-methoxybenzaldehyde, is a phenolic aldehyde with the molecular weight of 152.15 g/mol. Its functional groups compose of aldehyde, ether, and phenol. Vanillin can partially dissolve in water but absolutely dissolve in ethanol and methanol. In natural, it is a primary component in the vanilla bean. The compound can be chemically synthesized using electrophilic aromatic substitution reaction between guaiacol and glyoxylic acid to obtain vanillylmandelic acid which could be further converted to vanillin. Vanillin is used as a flavoring agent in foods, beverages, cosmetics and pharmaceuticals.

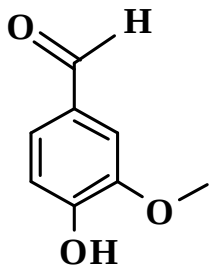

Figure 1.22 Chemical structure of vanillin

Citral

Citral, 3,7-dimethylocta-2,6-dienal, is a monoterpenoid alcohol which was widely found in essential oils of several plants. Its boiling point is around 230 ^{o}C and the molecular weight is 152.24 g/mol. Citral is insoluble in water but absolutely soluble in alcohol, ether and most common organic solvents. It is used in perfumery and flavoring. Citral also possesses antimicrobial activities.

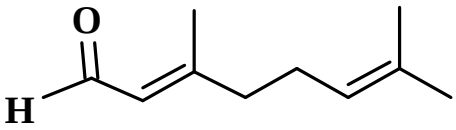

Figure 1.23 Chemical structure of citral

Research goals

The aim of this research is the fabrication of the thermoresponsive biopolymer for the controlled release of fragrances. The procedures of this research as follow:

1. Synthesis of methoxy-terminated poly(ethylene oxide) carboxylic acid (mPEO-COOH)
2. Synthesis of poly(ethylene oxide) grafted-chitosan (mPEO-CS)
3. Preparation of vanillidene-mPEO-CS and citralidene-mPEO-CS polymeric particles
4. Chemical structure and morphology characterization

5. Evaluation of aggregation-dissociation behavior
6. Investigation of thermally controlled release profiles

CHAPTER II
EXPERIMENTAL

2.1 Materials and chemicals

Chitosan (MW 30,000 Da, 85% deacetylated) was purchased from Seafresh Chitosan Lab Co., Ltd (Thailand). Succinic anhydride, citral, vanillin, and 1-ethyl-3-(3-dimethyllaminopropyl) carbodiimide hydrochloride (EDCI.HCL) were obtained from Acros organics (Geel Belgium). Pyridine and $ZnSO_4.7H_2O$ were purchased from CARLO ERBA (Val de Reuil, France). Polyethyleneglycol methyl ether (mPEG, MW 5000) was purchased from Fluka (Missouri, USA). 1-Hydroxybenzotriazole (HOBt) was recrystallized in MeOH and other chemicals were analytical grade.

2.2 Synthesis of methoxy-terminated poly(ethylene oxide) carboxylic acid

Polyethyleneglycol methyl ether (mPEG 5000, 10.00 g) was reacted with succinic anhydride (4.00 g, 20 mole equivalent to mPEG) in DMF (20 mL) with a catalytic amount (2 drops) of pyridine at 60^{o}C overnight to achieve methoxy-terminated poly(ethylene oxide) carboxylic acid (mPEO-COOH). The reaction was described in following Scheme 2.1. The obtained product was purified by dialysis against water using benzoylate dialysis tubing (MWCO 2000, Sigma-Aldrich, Missouri, USA) before drying by freeze dry method. Structural characterization of the product was achieved on a 400 MHz Varian mercury nuclear (^{1}H) magnetic resonance spectrometer (Varian Inc., Palo Alto, USA).

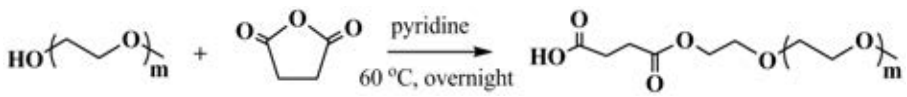

Scheme 2.1 Synthesis of mPEO-COOH

Methoxy-terminated poly(ethylene oxide) carboxylic acid (mPEO-COOH): yield = 60%. ^{1}H-NMR (D_2O, 400 MHz, δ, ppm): 2.51 (-COC**H$_2$**C**H$_2$**COOH); 4.11 (-OC**H$_2$**C**H$_2$**OCOCH$_2$CH$_2$COOH); 3.35-3.70 (-OC**H$_2$**C**H$_2$**OCH$_3$); 3.20 (-OCH$_2$CH$_2$OC**H$_3$**).

2.3 Synthesis of poly(ethylene oxide) grafted-chitosan (mPEO-CS)

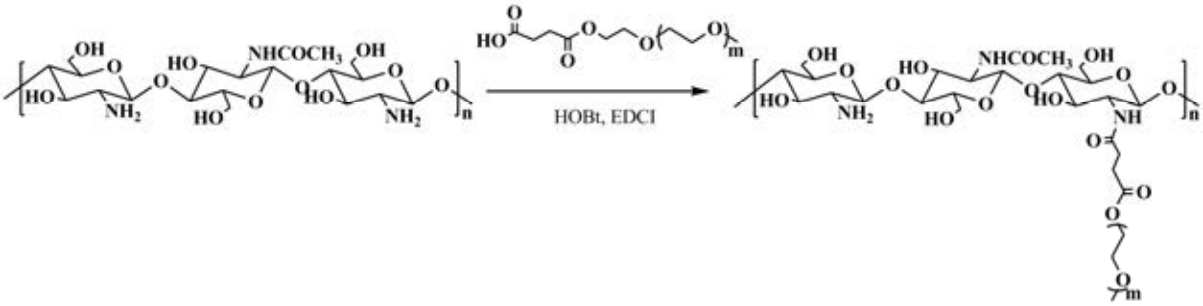

Scheme 2.2 Synthesis of mPEO-CS

Poly(ethylene oxide) grafted-chitosan (mPEO-CS) was synthesized by homogeneous coupling reaction in aqueous solution. Chitosan MW 3,000 (0.25 g, 1.53 mmole) was blended with HOBt (0.206 g, 1.53 mmole) followed with addition of deionized water (20 mL) and stirred until a clear solution was obtained. Next, aqueous solution of mPEO-COOH (0.765 g, 0.153 mmole, 10 mL) was added drop-wise, following with the addition of aqueous EDCI.HCl (0.293 g EDCI, 1.53 mmole and 10 ml water) solution. The mixture was stirred at room temperature for 24 h. The obtained solution was precipitated in excess acetone and yellow crude gel was achieved. The crude gel was filtered and washed by acetone followed with ethanol for several times and then dried under vacuum at ambient temperature. The product was characterized using Nuclear magnetic resonance (NMR) Varian mercury 400 MHz (Varian Inc., Palo Alto, USA). Attenuated Total Reflectance- Fourier transform infrared (ATR-FTIR) spectra were recorded with Nicolet 6700 FT-IR spectrometer (Thermo Electron Corporation, Madison, WI, USA) connected to a Continuμm^{TM}

infrared microscope equipped with a mercury-cadmium-telluride (MCT) detector. X-ray diffractrometer, Rigaku DMAX 2200/Ultima^{+} diffractometer (Rigaku International Corporation, Tokyo, Japan) operating with Cu Kα radiation at 40 kV and 30 mA, was used to characterize crystallinity of mPEO-CS.

Poly(ethylene oxide) grafted-chitosan (mPEO-CS): yield = 64%. ^{1}H-NMR (D_2O, 400 MHz, δ, ppm): 2.83-2.89 (-COC**H$_2$**C**H$_2$**COOH); 4.23 (-OC**H$_2$**C**H$_2$**OCOCH$_2$CH$_2$CONH); 3.34 (-OCH$_2$CH$_2$OC**H$_3$**);); 2.02 (-NHCOCH$_3$); 3.56-3.72 (-OC**H$_2$**C**H$_2$**OCH$_3$, H2', H3, H4, H5, and H6); 4.78 (H1); 3.07 (H2) (labeled in figure 1). ATR-FTIR (cm^{-1}): 3378 (N-H and O-H stretching), 2877 (C-H stretching), 1645 (C=O stretching of amide I), 1515 (N-H bending of amide II), 1343 (C-N stretching of amide III), 1731 (C=O stretching of ester), 1140 (C-O-C stretching) and 1090 (C-O stretching of glucosamine unit).

2.4 Preparation of imine-mPEO-CS

mPEO-CS (90 mg) was dispersed in 30 mL of deionized water before addition (drop-wise) of each perfumery aldehyde (vanillin and citral), which was dissolved in ethanol (3 mL), under high-intensity ultrasound (40 kHz) at room temperature for 4 h.

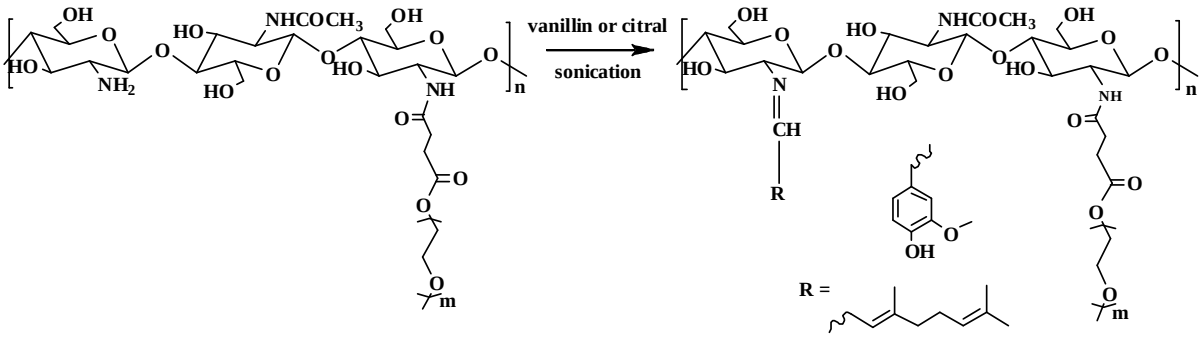

Scheme 2.3 Synthesis of imine-mPEO-CS

N,N′-vanillidene-mPEO-chitosan, ATR-FTIR (cm^{-1}): 3378 (N-H and O-H stretching), 2877 (C-H stretching), 1635 (C=N stretching of imine), 1731 (C=O

stretching of ester), 1140 (C-O-C stretching) and 1090 (C-O stretching of glucosamine unit).

N,N′-citralidene-mPEO-chitosan, ATR-FTIR (cm^{-1}): 3378 (N-H and O-H stretching), 2877 (C-H stretching), 1638 (C=N stretching of imine), 1731 (C=O stretching of ester), 1140 (C-O-C stretching) and 1090 (C-O stretching of glucosamine unit).

Hydrodynamic diameter of samples were acquired on a Zetasizer nanoseries instrument (Malvern Instrument, Worcestershire, UK) while morphological and aggregation-dissociation behavior images were achieved from JEM-2100 transmission electron microscope (JEOL, Tokyo, Japan) and confocal microscopes, Nikon Ti-E Inverted Microscope Confocal Nikon C1si-system (Nikon Corpopation, Tokyo, Japan) with differential interference contrast (DIC) mode, respectively. Moreover, scanning probe microscopic (SPM) images were obtained from Nanoscope IV scanning probe microscope (Veeco Metrology Group, New York, USA) analysis in tapping mode.

2.5 Optimization ratio of aldehydes

mPEO-CS suspension was prepared at concentration of 3.0 g/L. The suspension was divided into five parts. Each part containing 10 mL of the suspension was reacted with ethanolic solution of vanillin (10% v/v) under high intensity ultrasonication (40 kHz) at mass ratios of polymer to vanillin of 1:1, 2:1, 3:1, 4:1, and 5:1. Product from each reaction was subjected to ATR-FTIR spectroscopic analysis. The ratio having maximum amount of grafted-vanillin and minimum of free fragrant aldehyde was selected for next experiments. Similar experiment was carried out with citral in place of vanillin.

2.6 Evaluation of surface chemical composition

Samples with the optimized polymer to aldehyde ratio obtained from section 2.5 were subjected to X-ray photoelectron spectroscopic (XPS) analysis (Kratos AXIS Ultra DLD instrument equipped with a monochromatic Al Kα X-ray source (1486.6 eV), operated with X-ray source at 150 W (15 kV and 10 mA)(Kratos, Manchester, England). To acquire C 1s and N 1s high resolution spectra, the base pressure in analysis chamber and passed energy with energy steps 0.1 eV were $5x10^{-8}$ torr and 20 eV, respectively. For deconvolution, the hydrocarbon C 1s peak at 285 eV was used as binding energy (BEs) reference peak.

2.7 Investigation of phase transition profile

Transmittance of the suspension of imine-mPEO-CS with polymer concentration of 3.0 g/L in a presence of various concentrations of $ZnSO_4.7H_2O$ (0, 0.8, 0.9, and 1 M for vanillidene-mPEO-CS and 0, 1, 1.3, and 1.5 M for citralidene-mPEO-CS) were measured using UV-visible spectrophotometer, CARY 100 Bio UV-Vis spectrophotometer (Varian Inc., Palo Alto, USA), equipped with temperature controller. Samples were heated up from 25 to 80 ^{o}C followed with cooled down from 80 to 25 ^{o}C with a rate 1 ^{o}C/min.

2.8 Determination of critical micelle concentration

The 1000 μM of aliquot (10 mL) of pyrene solution was added into each clean test tube and dried under nitrogen, then 10 ml of citralidene-mPEO-CS in water (at various concentrations of 0.01, 0.1, 0.25, 0.35, 0.5, 0.6 g/L) were added. The samples were kept at room temperature overnight for equilibration. Then the samples were subjected to fluorescence spectroscopic analysis on PerkinElmer LS 55 Luminescence Spectrometer (PerkinElmer, Massachusetts, USA). Plot between ratio of fluorescent intensity at 372 to 382 nm and concentration of citralidene-mPEO-CS (g/L) was then

contructed and critical micelle concentration (CMC) was estimated from the interception of curve fitting between two slopes.

2.9 Hydrolysis of imine bond with temperature control

To investigate thermally controlled release profiles, suspension of vanillidene-mPEO-CS (30 mL) with polymer concentration 6.0 g/L was prepared, then phosphate buffer pH 1 (30 mL) and addition of $ZnSO_4.7H_2O$ (15.5 g) were added. Final concentrations of polymer and $ZnSO_4.7H_2O$ in the mixture were 3.0 g/L and 0.9 M, respectively. Whereas, citralidene-mPEO-CS was prepared with polymer concentration 3.0 g/L in deionized water (60 mL) and $ZnSO_4.7H_2O$ (25.9 g, 1.5 M) was added to it. Each uncovered vial containing 5 mL of the mixture was subjecting to the determination of vanillin or citral release with switching temperature every 2 days between 35 and 55 ^oC for vanillin and every 1 day between 30 and 40 ^oC for citral. The sample of vanillidene-mPEO-CS was collected on day 0, 2, 4, 6, 8, 10 whereas citralidene-mPEO-CS was collected on day 0, 1, 2, 3, 4, 5 by addition of 1.0 M HCl (1.0 mL) followed with addition of ethanol : H_2O (1 : 1) 15.0 mL for vanillin and hexane (15.0 mL) for citral. The collected vials were then capped with headspace aluminum crimp caps with PTFE/silicone septa. The mixtures in the vials were then subjected to UV-vis spectrophotometric analysis (Shimadzu Corporation, Kyoto, Japan) in order to quantitate aldehyde released.

2.10 Hydrolysis of imine bond with salt control

To demonstrate release profiles of both imine-mPEO-CS, at various salt concentration under constant temperature, the suspension of each imine-mPEO-CS in deionized water (200 mL) was prepared and divided into two parts, 100 mL each. The first part was added with $ZnSO_4.7H_2O$ (28.8 g, 1 M for vanillidene-mPEO-CS and 43.1 g, 1.5 M for citralidene-mPEO-CS) while no salt was added to the other part. Then the samples were transferred into vials (5.0 mL for each vial). Each vial containing 5.0 mL of sample was kept uncovered at 40 ^oC. Collection of the samples

was proceeded on day 0, 1, 2, 5, 8, 12, 15, 20, 26 for vanillidene-mPEO-CS while on day 0, 1, 2, 5, 7, 10, 15, 20 for citralidene-mPEO-CS with following method, 1 M HCl (1 mL) was added followed with addition of ethanol : H_2O (1 : 1) 15 mL for vanillin. Whereas, followed with addition of hexane (15 mL) for citral. Next, the vial was capped with headspace aluminum crimp caps, inserting with PTFE/silicone septa. Finally, each treated sample was subjected to UV-vis spectroscopic analysis for aldehyde quantification.

CHAPTER III
RESULTS AND DISCUSSION

Morinaga and coworkers [5] reported novel concept for controlling release of fragrance which was based on chemical derivatization and temperature-dependenced responsiveness and found that the self-assembly thermoresponsive polymers could control the release rate of the fragrance molecules which were grafted on the thermoresponsive amphiphilic polymeric chain. In this report, we demonstrated the same concept for controlling release of fragrances, however our system is fabricated from the biodegradable/biocompatible chitosan polymer using the reversible imine linkage between fragrant aldehydes and amino groups of the chitosan. Here the biocompatible polyethylene oxide was also grafted onto the chitosan to inherit thermoresponsive character to the polymer.

3.1 Synthesis and characterization of mPEO-COOH

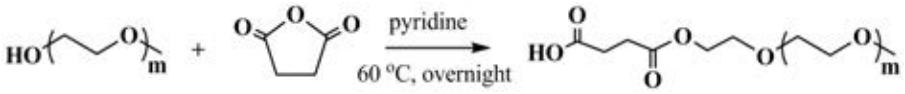

Scheme 3.1 Schematic representation of synthesis of mPEO-COOH

Methoxy-terminated poly(ethylene oxide) carboxylic acid (mPEO-COOH) was synthesized from reaction between polyethyleneglycol methyl ether and succinic anhydride at 60 ^{o}C, pyridine was used as catalyst. The product is white powder and well-dissolved in aqueous media. ^{1}H NMR spectrum of the product in D_2O is shown in Figure 3.1, protons at chemical shift 2.51 ppm represented methylene protons of succinyl group. This could imply that the succinyl group was successfully grafted on the polyethyleneglycol chain.

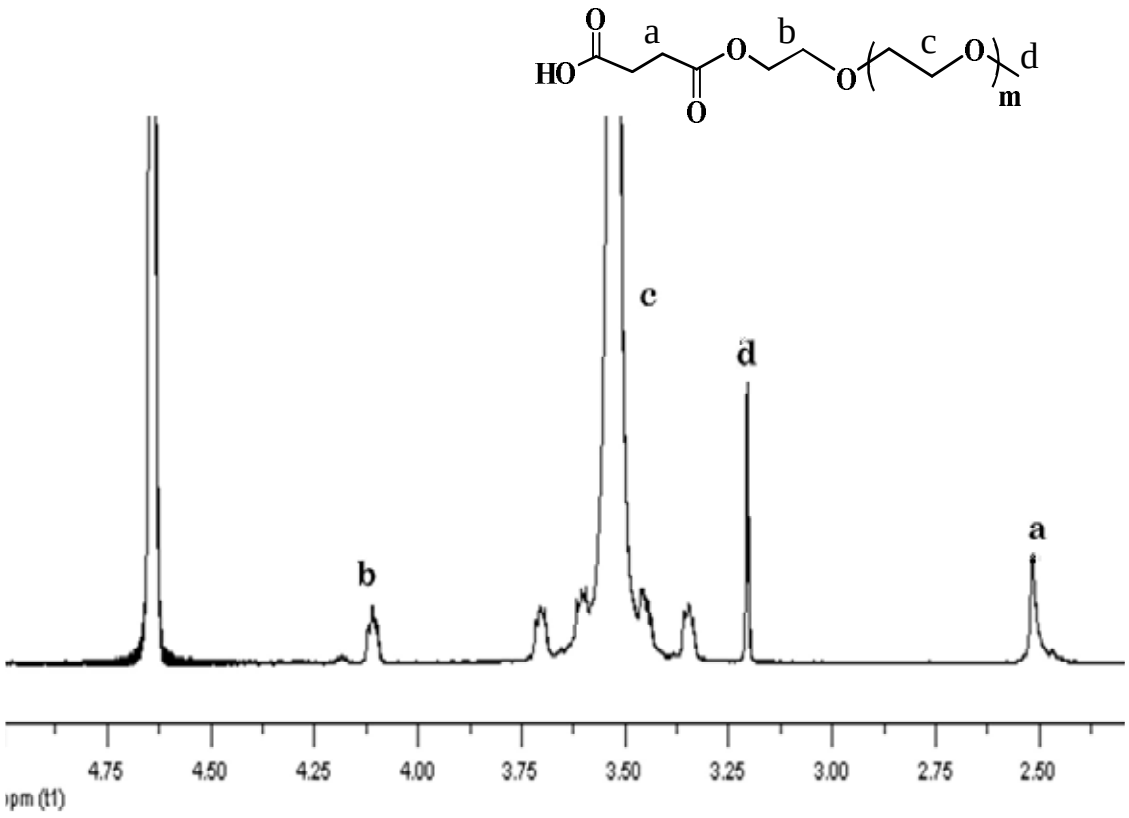

Figure 3.1 ^{1}H NMR spectrum of mPEO-COOH

3.2 Synthesis and characterization of mPEO-CS

Poly(ethylene oxide) grafted-chitosan (mPEO-CS) was synthesized by homogeneous coupling reaction between chitosan and mPEO-COOH in aqueous media (scheme 3.2). Appearance of product is light yellow solid (figure 3.2 (b)). ^{1}H NMR spectrum of mPEO-COOH (figure 3.1) showed methylene protons peak of succinyl group at 2.51 ppm which illustrated that mPEG was modified by succinylation. ^{1}H NMR spectrum of mPEO-CS (figure 3.2 (a)) showed methylene protons peak of mPEG moiety at 3.56-3.72 ppm. ATR-FTIR spectrum of mPEO-CS showed new absorption peak at 1731 cm^{-1} corresponding to C=O stretching of an ester bond and an increase of absorption peak at 2877 cm^{-1} corresponding to C-H stretching (Figure 3.3). These indicated that mPEO-COOH was grafted on amino group of chitosan. A mPEO-COOH substitution degree , which was evaluated from NMR spectroscopic method, was 0.168. Figure 3.4 showed XRD patterns of chitosan, mPEO-COOH, and mPEO-CS. Chitosan exhibited reflection peaks at 2-theta equal to

11 and 20° while 19 and 23° were observed for mPEG-COOH. The grafted mPEO-CS showed only two broad peaks at 19 and 23°, no peak at10° was observed. This indicated that bond formation between chitosan and mPEG-COOH disrupted packing of chitosan chain and led to the decrease of the crystallinity.

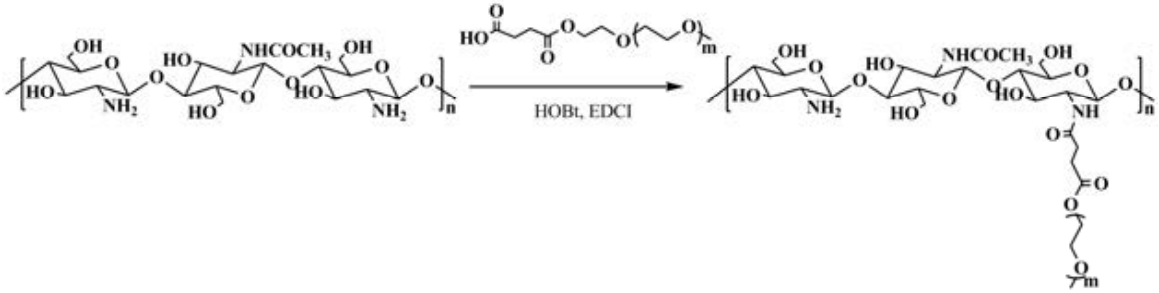

Scheme 3.2 Schematic representative of synthesis of mPEO-CS

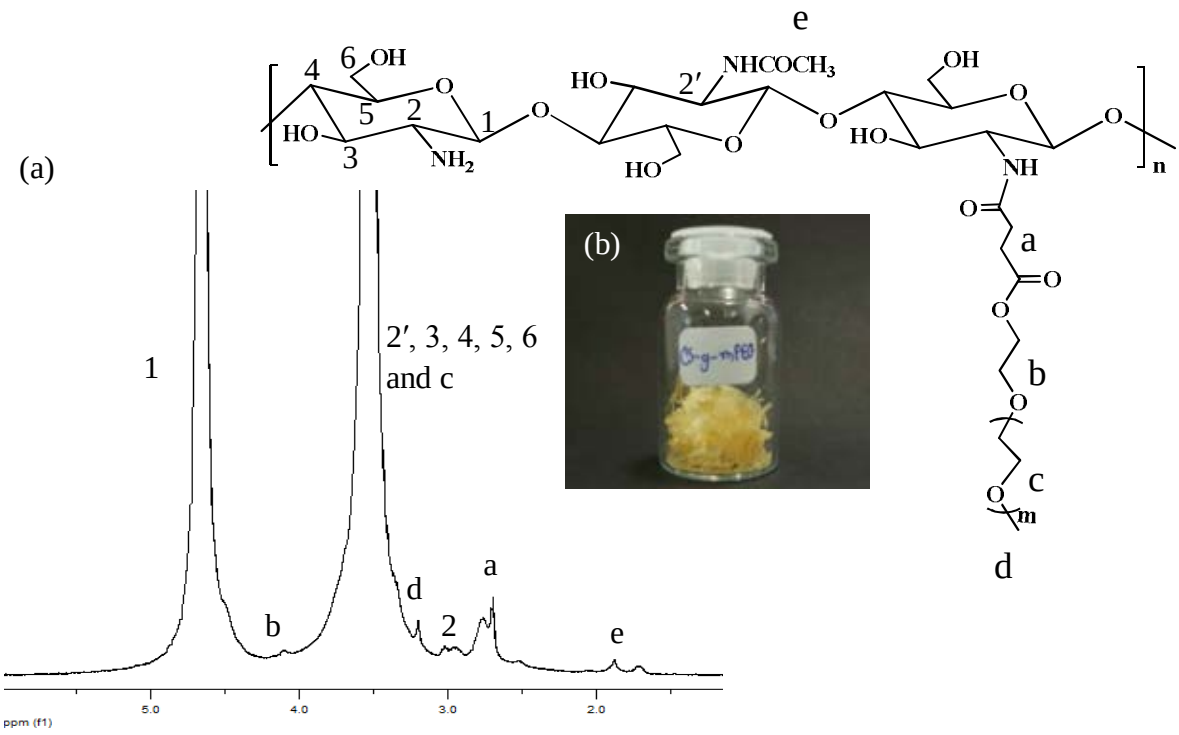

Figure 3.2 (a) ^{1}H NMR spectrum and (b) optical appearance of mPEO-CS

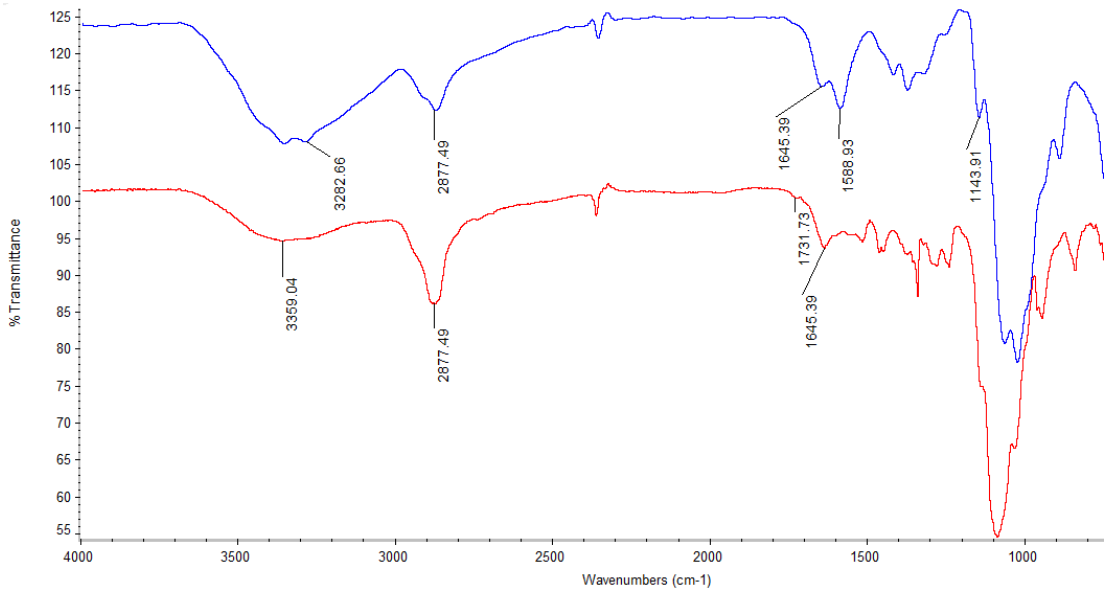

Figure 3.3 (top) ATR-FTIR spectra of chitosan and (bottom) mPEO-CS

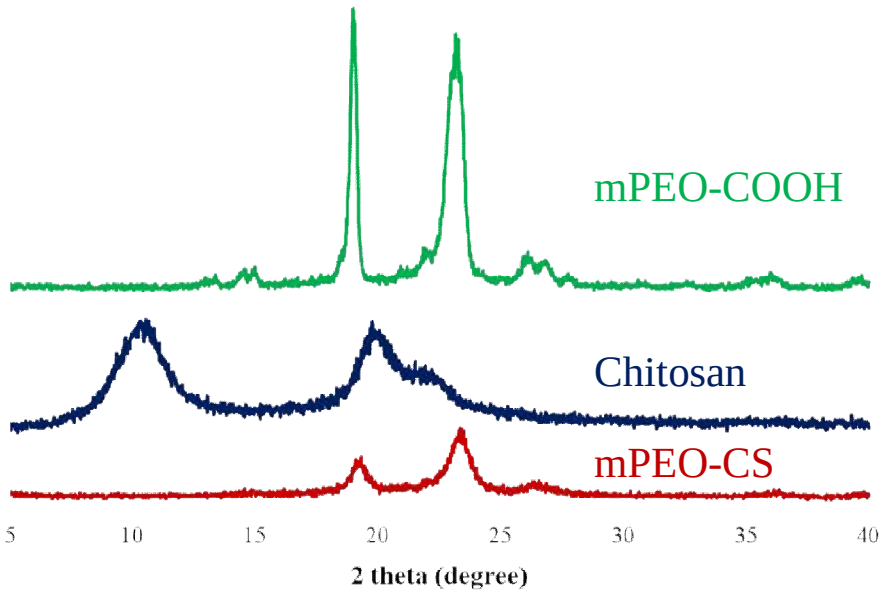

Figure 3.4 X-ray diffraction patterns of mPEO-COOH, chitosan and mPEO-CS

3.3 Preparation of imine-mPEO-CS

Two aldehydes, vanillin and citral, were used in the preparation of imine-mPEO-CS. ATR-FTIR spectrum of vanillidene-mPEO-CS showed new absorption peak at 1635 and 1509 cm^{-1} corresponding to C=N stretching vibration of the imine bond and C=C stretching vibration of aromatic, respectively. By subjecting the obtained vanilidene-mPEO-chitosan to acid hydrolysis followed with hexane extraction and quantifying the released vanillin by UV-vis absorption spectroscopy, the substitution degree of vanillin of 0.15 could be obtained. On the other hand, ATR-FTIR spectrum of citralidene-mPEO-CS (Figure 3.6) showed the absorption peak at 1638 and 1615 cm^{-1} which represented C=N stretching vibration of imine bond and C=C stretching vibration of aliphatic, respectively. Using similar hydrolysis/extraction and UV-vis absorption analysis as stated for the vanilidene-mPEO-chitosan, the degree of citral substitution of 0.12 could be obtained.

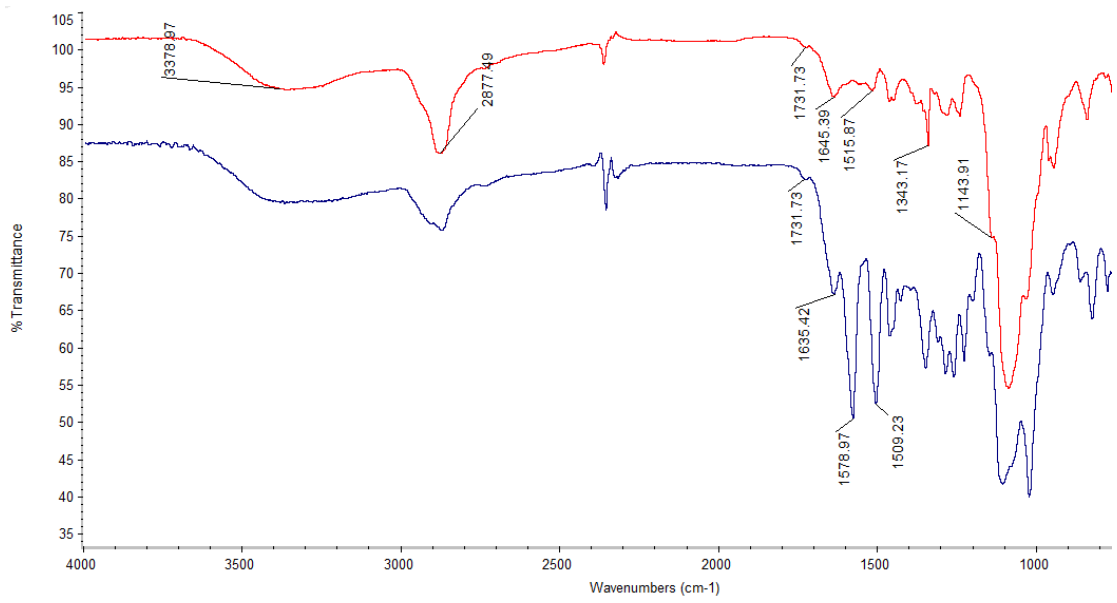

Figure 3.5 (top) ATR-FTIR spectra of mPEO-CS and (bottom) vanillidene-mPEO-CS

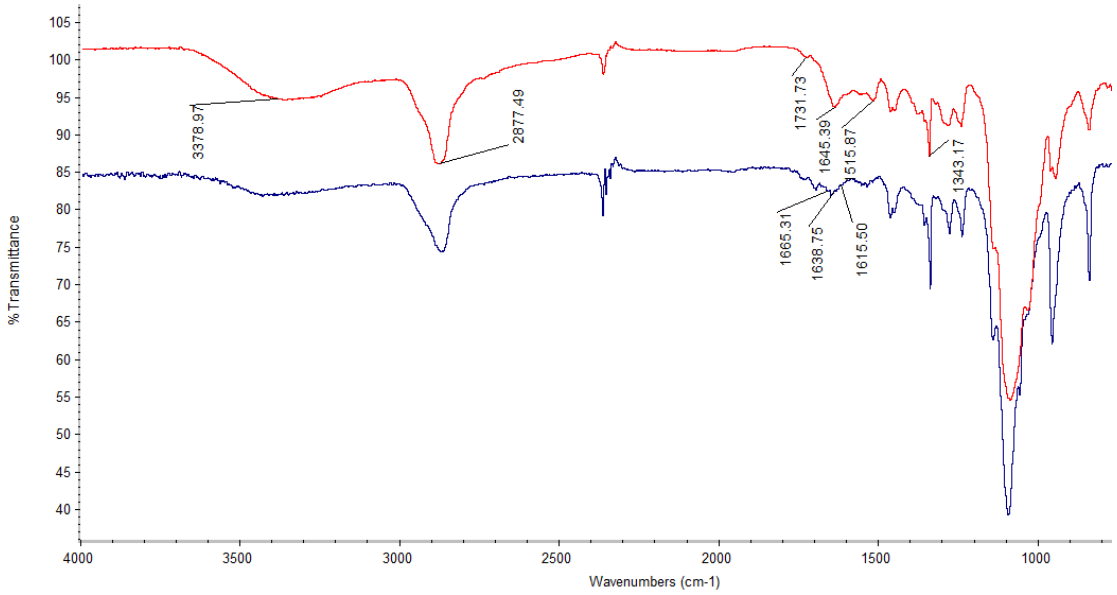

Figure 3.6 ATR-FTIR spectra of (top) mPEO-CS and (bottom) citralidene-mPEO-CS

3.4 Optimization ratio of perfumery aldehydes

The optimum ratio of fragrant aldehyde to polymer was evaluated by performing ATR-FTIR spectroscopic analysis on the products obtained from reaction of various ratios between the two starting materials. As was described in section 3.3, the absorption peak at 1635 and 1638 cm^{-1} assignable to C=N stretching of imine bond in vanillidene-mPEO-CS and citralidene-mPEO-CS, respectively, and absorption peak at 1668 cm^{-1} represented C=O stretching of free aldehyde, could be observed. The analysis revealed disappearance of the free aldehyde absorption peak at weight ratio of 4:1. Therefore, this ratio was used to prepare vanilidene-mPEO-CS with maximum vanillidene substitution without any free vanillin left in the system. In the case of citralidene-mPEO-CS, the optimum weight ratio of polymer to citral was 3:1 (Figure 3.8).

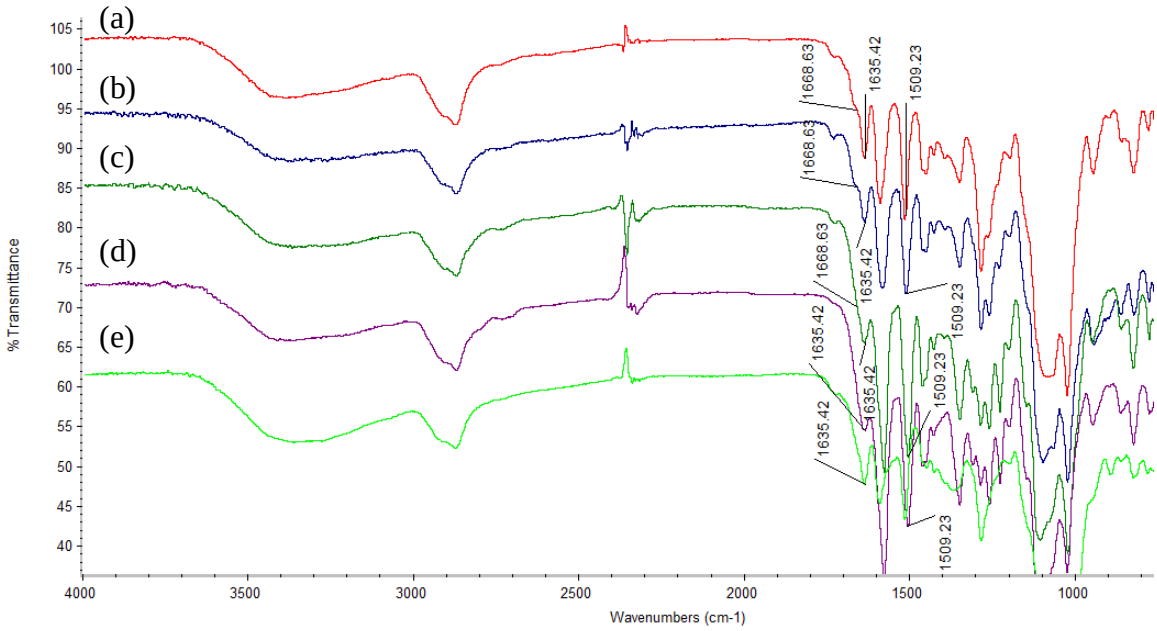

Figure 3.7 ATR-FTIR spectra of vanillidene-mPEO-CS with weight ratio of polymer to vanillin (a) 1:1, (b) 2:1, (c) 3:1, (d) 4:1, and (e) 5:1

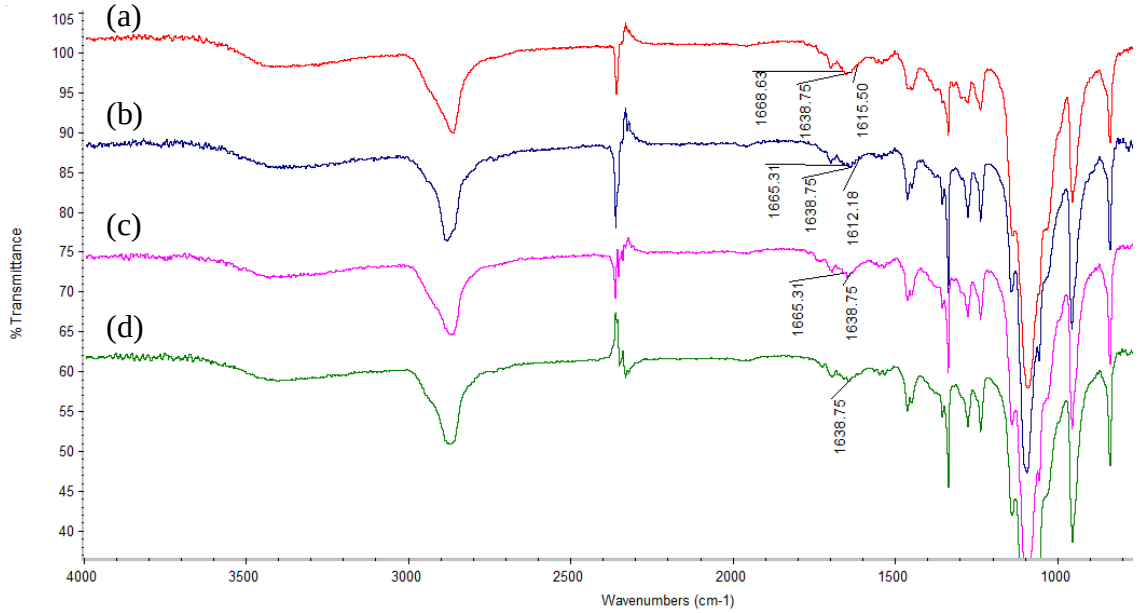

Figure 3.8 ATR-FTIR spectra of citralidene-mPEO-CS with weight ratio of polymer to citral (a) 1:1, (b) 2:1, (c) 3:1, and (d) 4:1

3.5 Critical aggregation concentration

Critical aggregation concentration of citralidene-mPEO-CS was determined using fluorescence spectroscopy by measuring pyrene probe. As seen in the Figure 3.9, graph was plotted between ratio of fluorescence emission intensity at wavelength 372 nm (I_{372}) and 382 nm (I_{382}) versus concentration of the polymer for 0.01, 0.1, 0.25, 0.35, 0.5, 0.6 g/L. The graph demonstrated the decrease in I_{372}/I_{382} ratio with the increase in the polymer concentration. When the polymer concentration was low, no aggregates of polymer could be formed thus environment of pyrene would be hydrophilic (no hydrophobic interior of any self-assembled architecture to associate with). In contrast, when the polymer concentration was increased over 0.35 g/L, polymer could form into polymeric aggregates, so pyrene molecules could move into the hydrophobic core of the micellar aggregates. Therefore, pyrene's environment would change to the hydrophobic one. The critical micelle concentration of citralidene-mPEO-CS was 0.47 g/L as determined from the sudden change in the I_{372}/I_{382} ratio which resulted from the change in the pyrene environment as described.

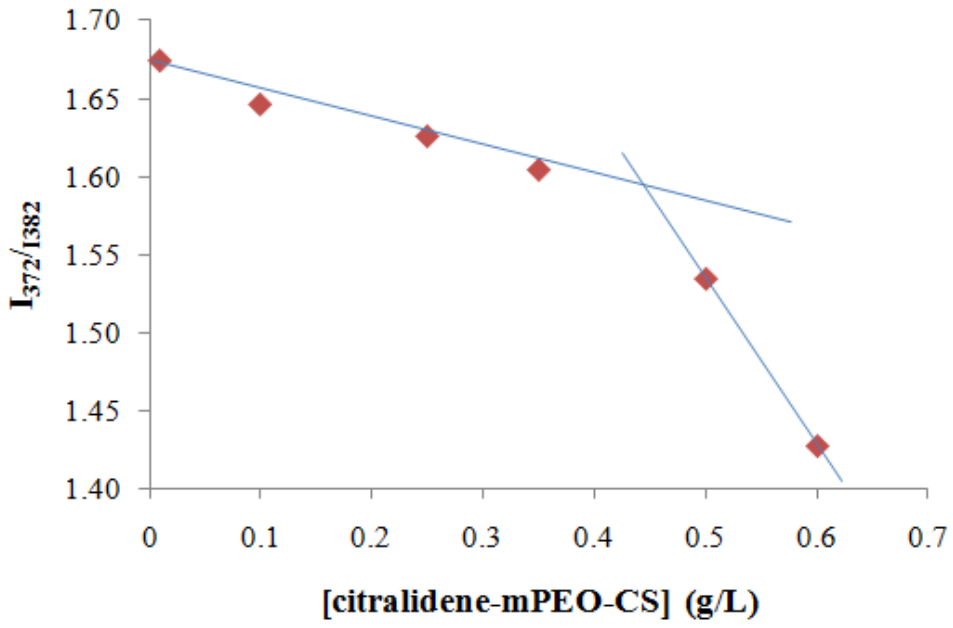

Figure 3.9 The plot between concentrations of citralidene-mPEO-chitosan versus the ratios of fluorescent intensisty at 372 and 382 nm, critical micellar concentration of citralidine-mPEO-chitosan determined from the graph was 0.47 g/L

3.6 Size and morphological characterization

The suspension of vanillidene-mPEO-CS and citralidene-mPEO-CS was prepared in aqueous media and morphology was observed using transmission electron microscopy (TEM) and scanning probe microscopy (SPM). Spherical shape could be clearly seen in TEM photographs of (Figure 3.11). Their SPM images (figure 3.12) indicated that imine-mPEO-CS particles was different from the bulk mPEO-CS. Dynamic light scattering technique was used to determine hydrodynamic diameter (mean value±S.D.) of the products which were ~ 452.03±46.4 (PDI of 0.345±0.07) and 306.67±51.4 (PDI of 0.427±0.03) nm for vanillidene-mPEO-CS and citralidene-mPEO-CS, respectively (Table 3.1 and Figure 3.10). The spherical sizes of non-hydrated vanillidene- and citralidene-mPEO-CS observed by TEM were less than the hydrated one, indicating swelling of the particles in water.

Table 3.1 Hydrodynamic diameter of mPEO-CS and both imine-mPEO-CS

Samples	**Hydrodynamic diameter**		**Zeta potential**
	(nm)	**PDI**	**(mV)**
mPEO-CS	577.67±15.04	0.492±0.07	+28.3±0.35
Vanillidene-mPEO-CS	452.03±46.4	0.345±0.07	+24.9±0.21
Citralidene-mPEO-CS	306.67±51.4	0.427±0.03	+24.3±0.32

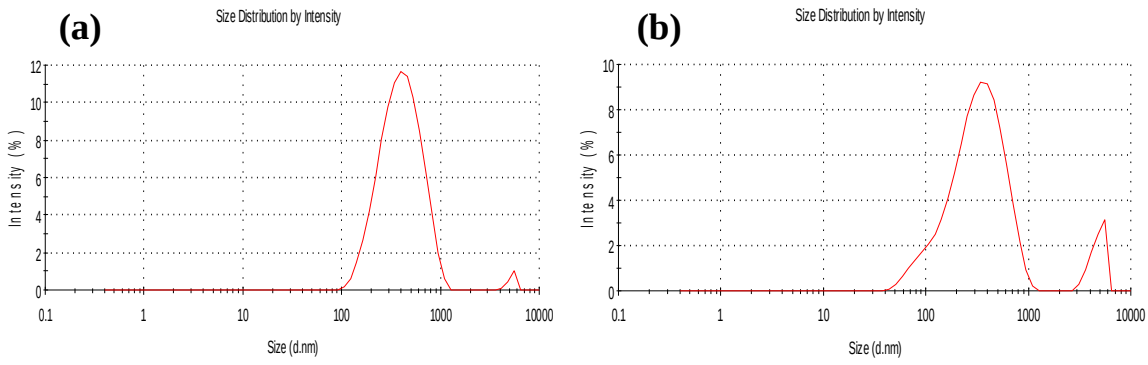

Figure 3.10 Size distribution curves of (a) vanillidene-mPEO-CS and (b) citralidene-mPEO-CS

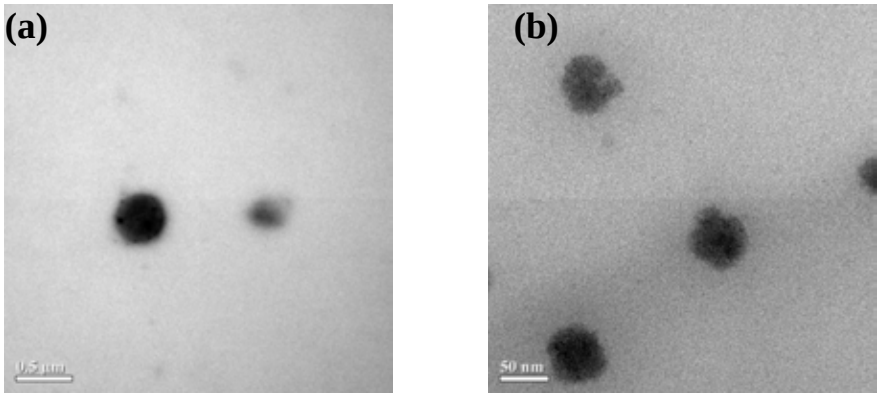

Figure 3.11 TEM photographs of (a) vanillidene-mPEO-CS and (b) citralidene-mPEO-CS

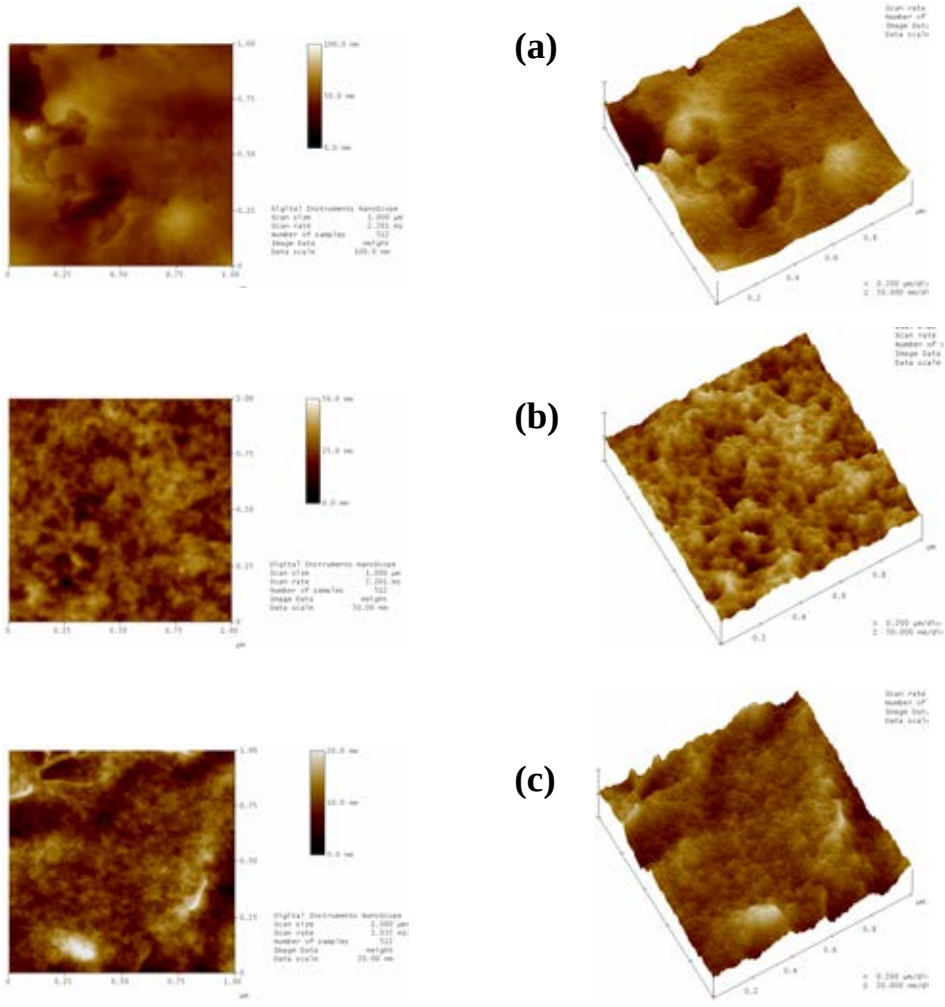

Figure 3.12 SPM images of (a) mPEO-CS, (b) vanillidene-mPEO-CS and (c) citralidene-mPEO-CS

3.7 Surface composition determination

The chemical composition at the surface of the self-assembled mPEO-CS was determined using X-ray photoelectron spectroscopy (XPS), which is a spectroscopic technique for analysis the surface composition of a solid sample at less than 8 nm depth from the surface. This technique was used to confirm position of the grafted imine bond which should embed inside of the sphere because of its hydrophobicity. In order to prove this assumption, the imine peak should not be observed.

The binding energy (BE) values of the C 1s and N 1s core-level spectra for all products are described below:

Chitosan(Figure 3.13 (a))

The XPS C 1s core-level spectrum of chitosan could be deconvoluted into three peaks [41] with BE's of 284.7, 286.1, 287.5 eV, attributable to C-H, C-OH, and O-C-O/NH-C=O, respectively. While, the N 1s core-level spectrum exhibited two peaks at BE's of 399.4 and 400.2 eV, assignable to -NH_2 and –NH-C=O, respectively.

mPEO-CS (Figure 3.13 (b))

mPEO-CS showed the new peak in the C 1s core-level spectrum at BE's of 288.4 eV, corresponding to O=C-O (from the ester bond in polyethyleneglycol chain). In both C 1s and N 1s core-level spectra, there was, moreover, new peaks at BE's of 285.5 and 398.6 eV, assignable to C-N and N=N bond, respectively, which belonged to contaminated-coupling agent, HOBt.

Non-self-assembled vanillidene-CS (Figure 3.13 (c))

The peaks observeable only in the non-self-assembled vanillidene-CS was at BE of 285.4 eV in C 1s core-level spectrum and 399.5 eV in N 1s core-level spectrum, corresponded to carbon and nitrogen species of C=N, respectively. Thus it was confirmed here that the imine bond of the non-self-assembled imine-CS could be observed on the surface.

Self-assembled vanillidene-mPEO-CS (Figure 3.13 (d))

The C 1s core-level spectrum of self-assembled vanillidene-mPEO-CS could be curve-fitted into four peaks with BE's at about 284.5, 286.1, 287.5, and 288.3 eV, attributable to C-H, C-OH, O-C-O/NH-C=O, and O=C-O, respectively. However, the imine functionality could not be observed. in both the C 1s and the N 1s core-level spectra, indicating that the imine functionality (observed in IR) was not at the surface,

thus, supporting the self-assembling model in which the grafted aldehyde and ketone should be at the particles' cores.

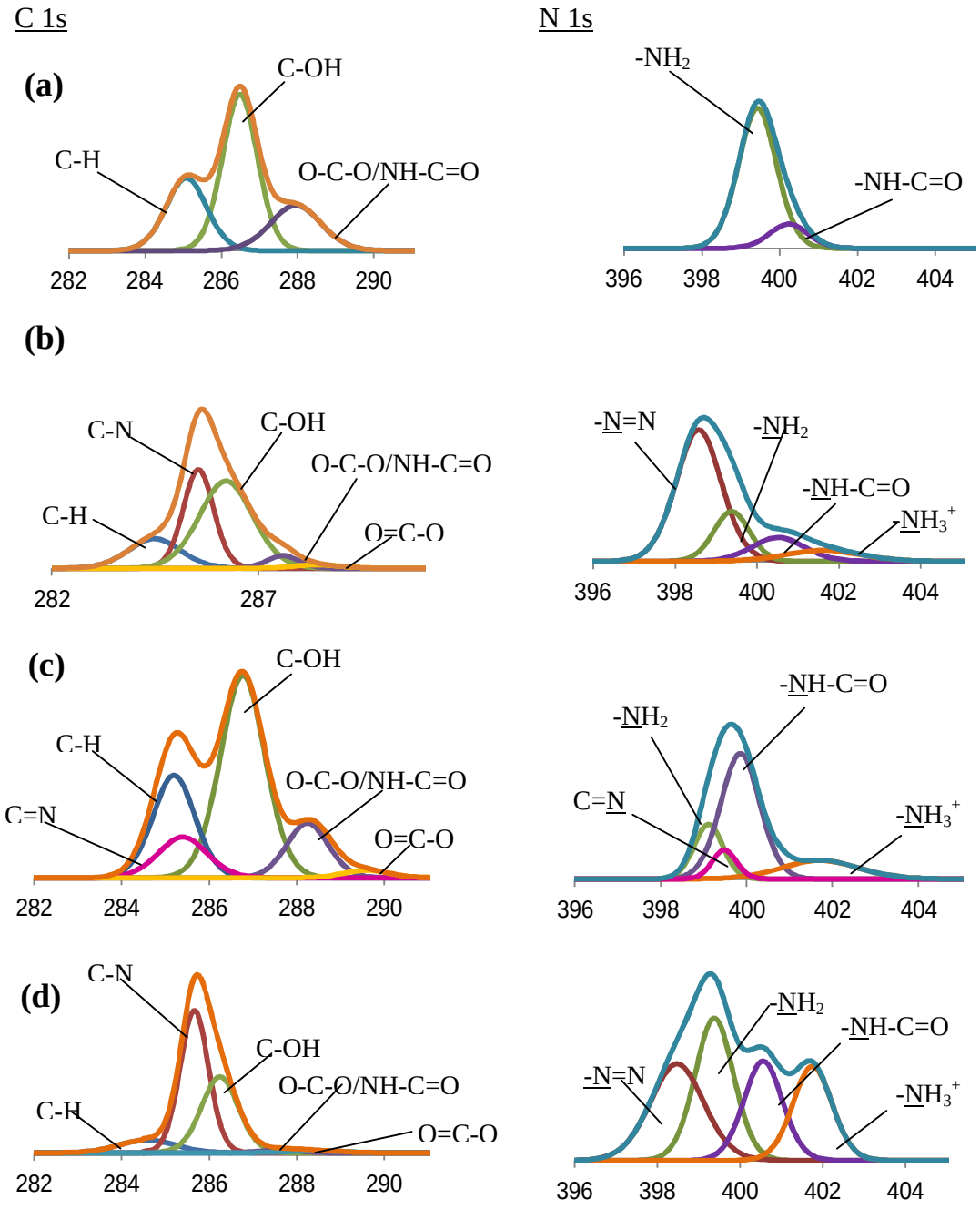

Figure 3.13 The deconvoluted C 1s and N 1s XPS spectra of (a) chitosan, (b) mPEO-CS, (c) non-self-assembled vanillidene-CS and (d) self-assembled vanillidene-mPEO-CS

3.8 Phase transition behavior of imine-mPEO-CS

Vanillidene-mPEO-CS suspension (3 g/L) with $ZnSO_4.7H_2O$ (0, 0.8, 0.9 and 1 M) and citralidene-mPEO-CS suspension (3 g/L) with $ZnSO_4.7H_2O$ (0, 1, 1.3 and 1.5 M) were measured to investigate temperature dependence of aggregation-dissociation using UV-visible spectrophotometer equipped with temperature controller. A transparent suspension of sample was heated from 25 ^oC to 80 ^oC before cooled down to 25 ^oC. Then, percent of transmittance was plotted against temperature (figure 3.14). For vanillidene-mPEO-CS with 0 M of $ZnSO_4.7H_2O$ the percent of transmittance did not change in this temperature range. However, the transmittances suddenly decreased at 55, 45, and 35 ^oC by the addition of 0.8, 0.9 and 1 M $ZnSO_4.7H_2O$, , respectively. In a similar fashion, the citralidene-mPEO-CS suspension with 0 M of $ZnSO_4.7H_2O$ showed no change in the percent transmittance in the tested temperature range. However, in the presence of 1, 1.3, and 1.5 M $ZnSO_4.7H_2O$, the transmittances suddenly decreased at 65, 43 and 35 ^oC, respectively. The temperature values which showed the sudden change were the Lower Critical Solution Temperature (LCST) of the system. The sudden change indicated the switch from associated particles at the temperatures below LCST to dissociated particles at the temperatures above the LCST. The change thus corresponded to the switch from big particles (association of many nanoparticles) which could reflect light effectively to the small dissociated particles that could reflect light less effectively.

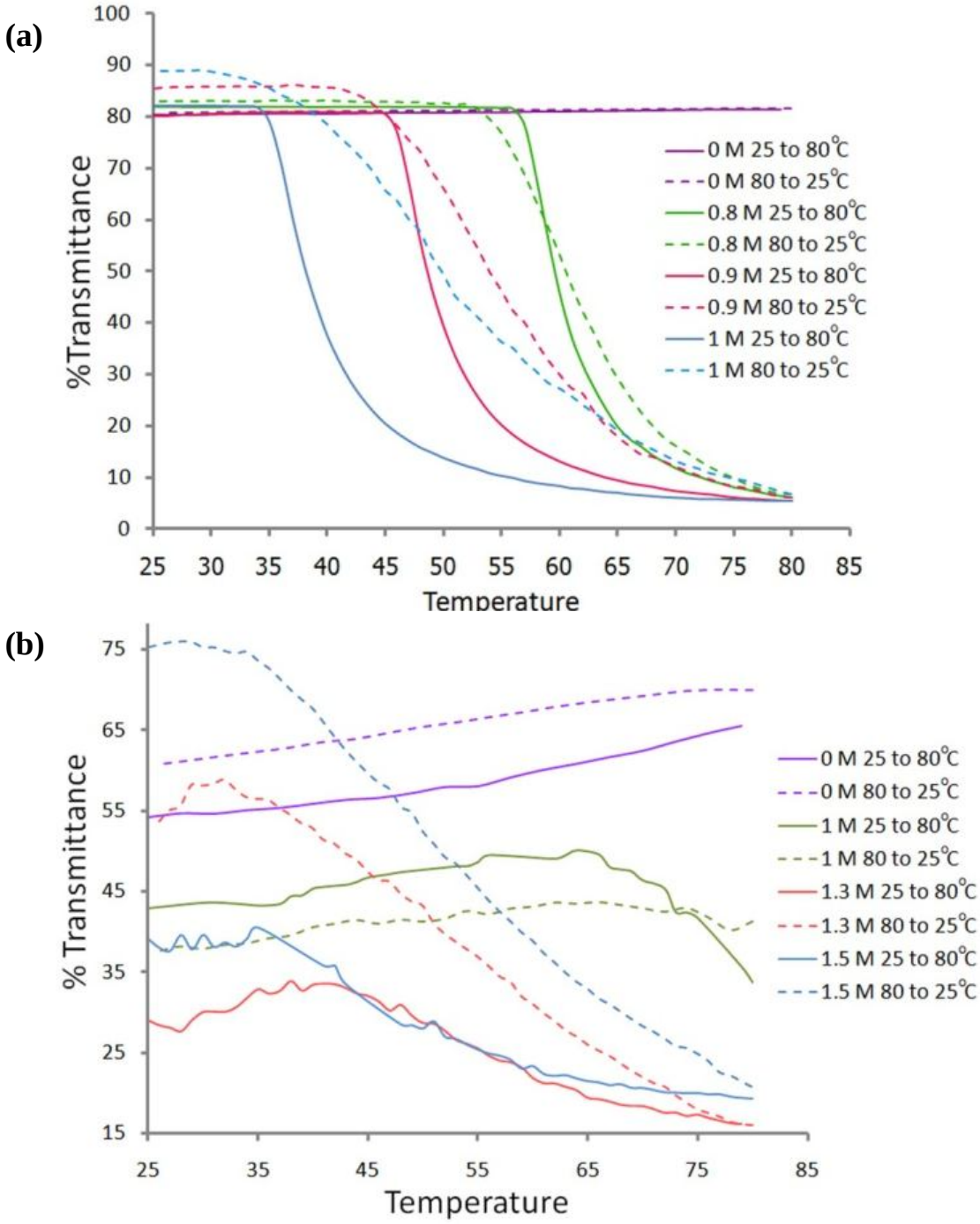

Figure 3.14 Phase transition profiles of (a) vanillidene-mPEO-chitosan and (b) citralidene- mPEO-chitosan at various $ZnSO_4$ concentrations

3.9 Temperature dependence of aggregation-dissociation behavior of imine-mPEO-CS nanoparticles

Confocal laser fluorescent microscope with differential interference contrast mode was used to demonstrate phase transition behavior of the self-assembled polymeric micelles of vanillidene-mPEO-CS and citralidene-mPEO-CS at the polymer concentration of 3 g/L in the presence of 0.9 and 1.5 M of $ZnSO_4.7H_2O$, respectively. When temperature was below LCST, vaillidene-mPEO-CS particles (Figure 3.15 (a)) and citralidene-mPEO-CS particles (Figure 3.15 (c)), dissociated as water molecules could well-hydrate the hydrophilic chains of the mPEO corona. In contrast, when the temperature reached the LCST, aggregation of particles could be observed (Figure 3.15 (b, d)). The aggregation was caused by the de-hydration of water molecules along the mPEO corona of the particles, leading to increased interaction among mPEO chains from the same and different particles.

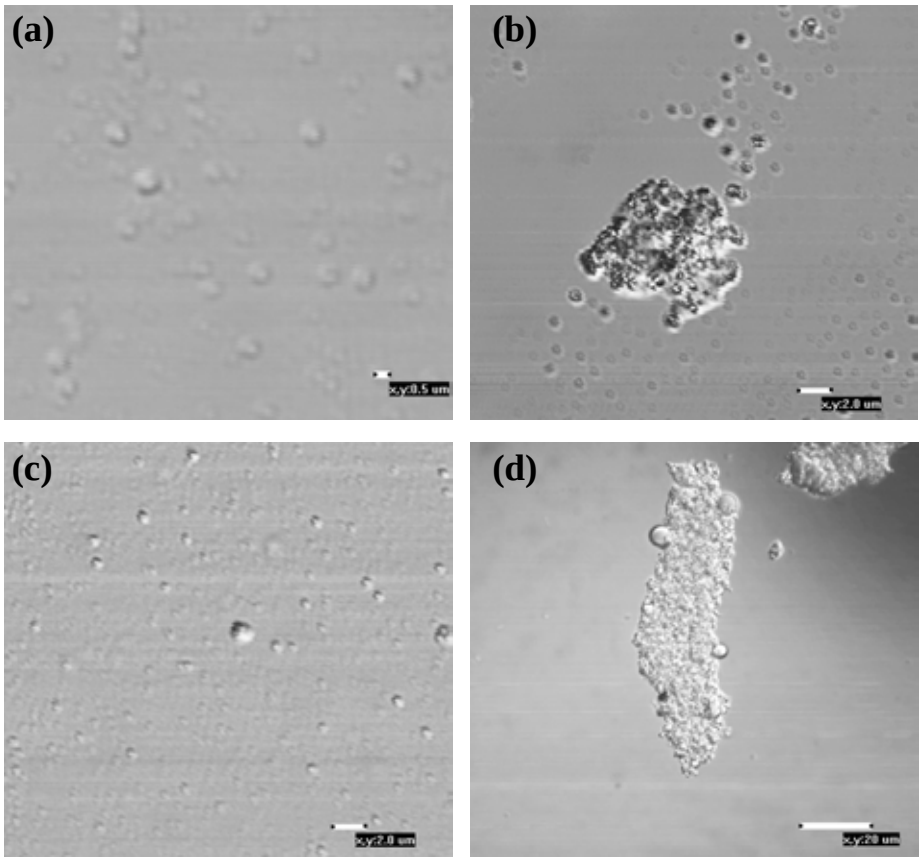

Figure 3.15 Morphology of vanillidene-mPEO-chitosan with 0.9 M $ZnSO_4$ at temperature (a) below LCST and (b) above LCST, and citralidene-mPEO-chitosan with 1.5 M $ZnSO_4$ at temperature (c) below LCST and (d) above LCST

3.10 Thermally controlled release of imine-mPEO-CS

As described in the previous section, the self-assembled polymeric nanoparticles could be in the aggregated or dissociated states depending on the temperature. Here, we reported investigation of thermally controlled release profiles of vanillidene-mPEO-CS and citralidene-mPEO-CS in the presence of $ZnSO_4.7H_2O$ (0.9 M for vanillidene-mPEO-CS and 1.5 M for citralidene-mPEO-CS). Our idea was that hydrolysis of imine bond to release out the fragrant aldehydes should be fast when the particles were dissociated as the water molecules could more easily diffuse into the particles' core where the imine bonds situated. In contrast, when the particle associated, the imine hydrolysis should be halt as no water could get into the imine sites. As seen in figure 3.16 and 3.17, rate of release of both vanillin and citral from mPEO-CS nanoparticles at temperature above LCST (55 and 40 ^{o}C for vanillin and citral, respectively) were more slowly than those at the temperature below LCST. Furthermore, the release of vanillin from vanillidene-mPEO-CS particles during their dissociated state was obviously slower than that of citral-mPEO-CS. This may be the effect of molecular structure, i.e., vanillin possesses aromatic ring that can allow the delocalization of electron to the imine linkage, leading to stronger imine bond. Therefore, the hydrolysis of vanillin' imine bond is more difficult than that in the case of citral.

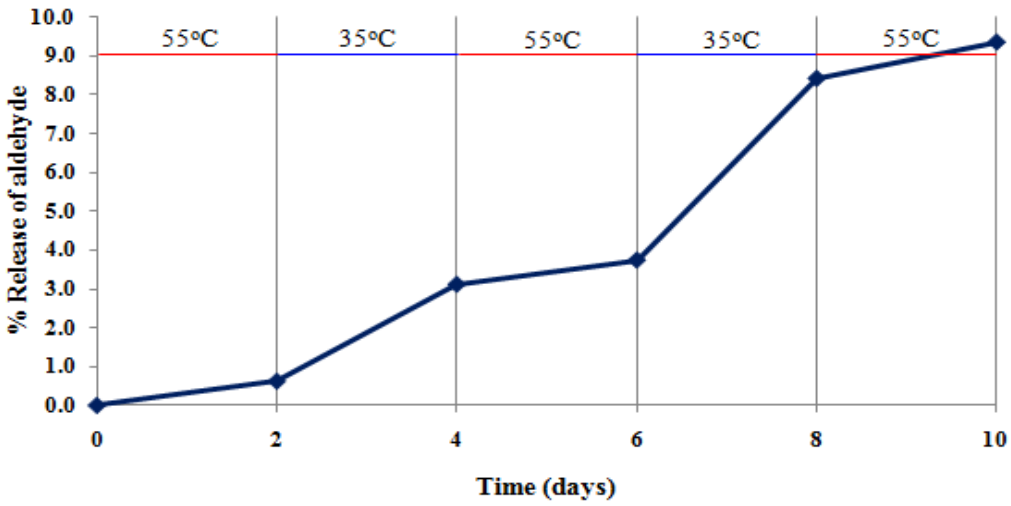

Figure 3.16 Thermally controlled release profile of vanillidene-mPEO-CS

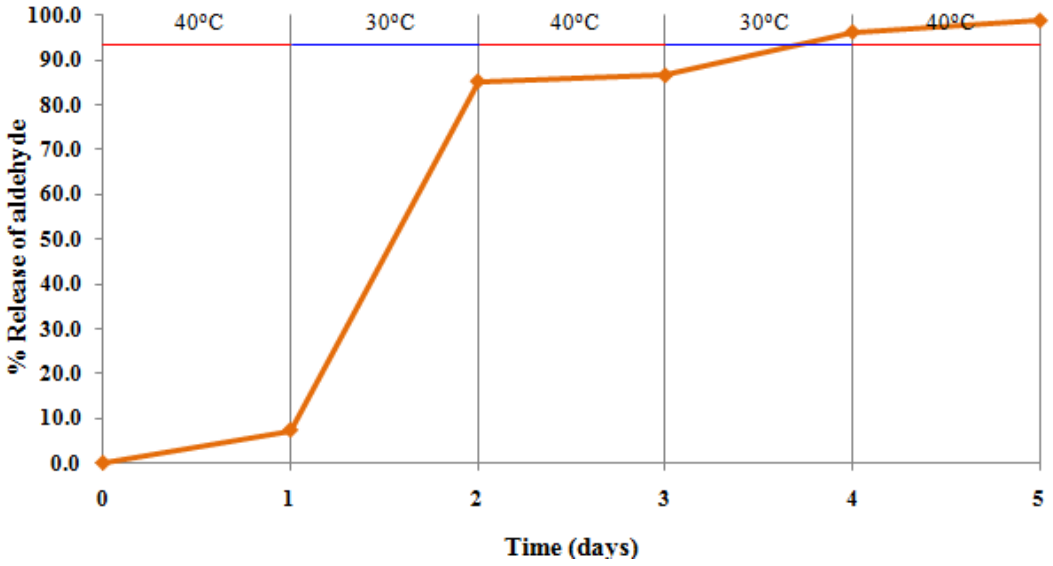

Figure 3.17 Thermally controlled release profile of citralidene-mPEO-CS

3.11 Controlling the release of imine-mPEO-CS by adjusting salt concentration

Even at a constant temperature, the release of fragrant aldehyde could be controlled by adjusting salt concentration. This is because the LCST was dependent not only on temperature but also on the concentration of salt in the system. Presence of salt in the system draws the water molecules away from the PEO chains by forming into more stable hydrated ions in the system. This automatically lowers the LCST of the polymer in that system. In this report, $ZnSO_4.7H_2O$ was used for adjusting LCST. Therefore, the release of the aldehydes could be controlled by adjusting concentration of $ZnSO_4.7H_2O$. The results shown below illustrate the difference of perfumery aldehyde release rate between the conditions with and without $ZnSO_4$ at a constant temperature.

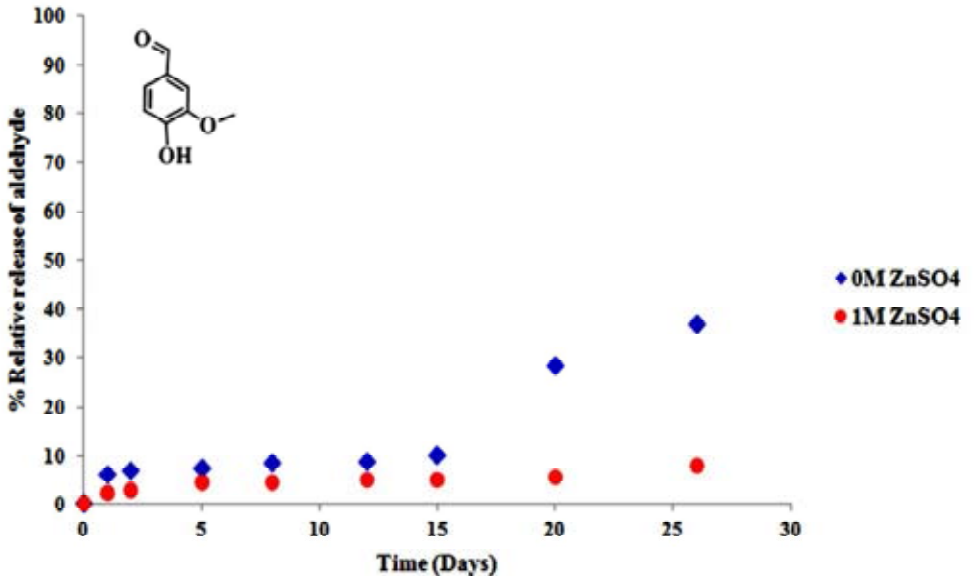

Figure 3.18 Release profile of vanillidene-mPEO-CS with and without 1 M $ZnSO_4$ at 40 ^{o}C

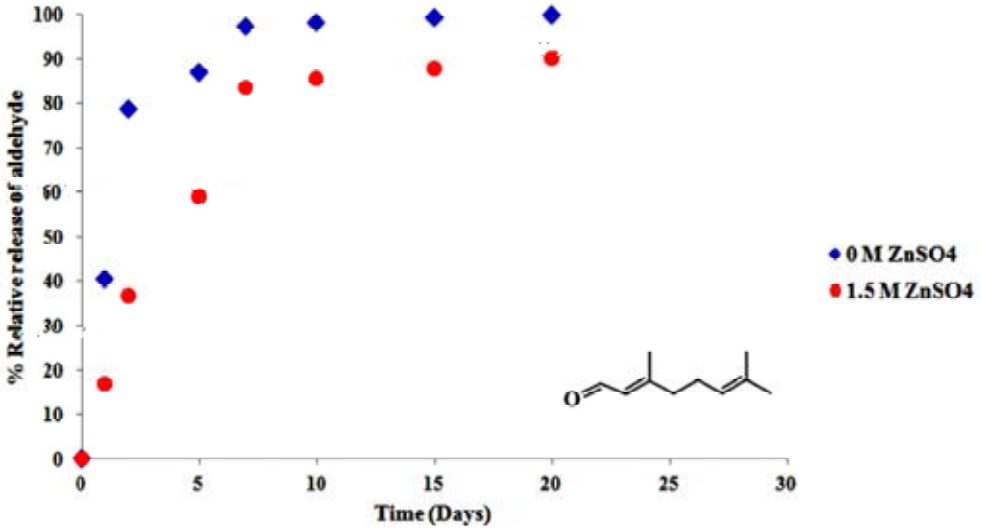

Figure 3.19 Release profile of citralidene-mPEO-CS with and without 1.5 M $ZnSO_4$ at 40 ^{o}C

As seen in the Figures, the percent release of vanillin and citral from vanillidene-mPEO-CS and citralidene-mPEO-CS, respectively, with the addition of $ZnSO_4.7H_2O$ were more slowly comparing to the same system with no salt present. It is found that the molecular structure of the grafted fragrant aldehyde affected the rate of release. Vanillin possesses more hydrophobicity than citral, so vanillidene-mPEO-CS nanoparticles is more hydrophobic than citralidene-mPEO-CS. This means water molecule could penetrate difficultly into vanillidene-mPEO-CS nanospheres. Therefore, the release rate of vanillidene-mPEO-CS was more slowly than citralidene-mPEO-CS.

CHAPTER IV
CONCLUSION

Thermoresponsive biopolymeric particle for controlled release of fragrances could be successfully fabricated. Vanillin and citral were grafted on the thermoresponsive copolymers, poly(ethylene oxide) grafted-chitosan (mPEO-CS, %DG = 16.8%) with %DG for 15 and 12%, respectively. The materials could self-assemble in aqueous media into particles with spherical shape. TEM photographs showed the estimated non-hydrated particle size of less than 1 μm for both vanillin and citral derivative. XPS high resolution spectral analysis confirmed that the position of grafted aldehydes were at the particles' core. The system showed thermally controlled release of the grafted fragrances in the presence of $ZnSO_4.7H_2O$; vanillidene-mPEO-chitosan with 0.8, 0.9, and 1 M $ZnSO_4$ showed the LCST at 55, 45 and 35^oC, respectively while citralidene-mPEO-chitosan with 1, 1.3 and 1.5 M $ZnSO_4$ showed the LCST at 65, 43 and 35^oC, respectively. The release of aldehydes could be thermally controlled in a switching manner. Release of vanillin with 0.9 M and citral with 1.5 M of $ZnSO_4$ was similar, minimal release could be obviously observed at the temperature above the LCST and significant release at the temperature below the LCST. Furthermore, the LCST of the system could be also selected by adjusting the salt concentration; an increase of salt concentration can reduce the LCST. Therefore, we successfully synthesized thermoresponsive chitosan polymer using poly(ethylene glycol) as a thermoresponsive moiety for the controlled release of fragrances. Moreover, we also successfully designed the thermo-switching controlled release system which is a completely biocompatible system for the release of fragrances.

REFERENCES

[1] Herrmann, A., Controlled release of volatiles under mild reaction conditions: from nature to everyday products. *Angewandte Chemie International Edition* 46, 31 (2007): 5836-5863.

[2] Berthier, D.; Trachsel, A.; Fehr, C.; Ouali, L.; Herrmann, A., Amphiphilic polymethacrylate- and polystyrene-based chemical delivery systems for damascones. *Helvetica Chimica Acta* 88, 12 (2005): 3089-3108.

[3] Berthier, D. L.; Paret, N.; Trachsel, A.; Herrmann, A., Influence of the backbone structure on the release of bioactive volatiles from maleic acid-based polymer conjugates. *Bioconjugate Chemistry* 21, 11 (2010): 2000-2012.

[4] Yang, Y.; Wahler, D.; Reymond, J.-L., β-amino alcohol properfumes. *Helvetica Chimica Acta* 86, 8 (2003): 2928-2936.

[5] Morinaga, H.; Morikawa, H.; Wang, Y.; Sudo, A.; Endo, T., Amphiphilic copolymer having acid-labile acetal in the side chain as a hydrophobe: controlled release of aldehyde by thermoresponsive aggregation−dissociation of polymer micelles. *Macromolecules* 42, 6 (2009): 2229-2235.

[6] Kumar, M. N. V. R.; Muzzarelli, R. A. A.; Muzzarelli, C.; Sashiwa, H.; Domb, A. J., Chitosan chemistry and pharmaceutical perspectives. *Chemical Reviews* 104, 12 (2004): 6017-6084.

[7] Fangkangwanwong, J.; Akashi, M.; Kida, T.; Chirachanchai, S., One-pot synthesis in aqueous system for water-soluble chitosan-graft-poly(ethylene glycol) methyl ether. *Biopolymers* 82, 6 (2006): 580-586.

[8] Yoksan, R.; Chirachanchai, S., Amphiphilic chitosan nanosphere: Studies on formation, toxicity, and guest molecule incorporation. *Bioorganic & Medicinal Chemistry* 16, 5 (2008): 2687-2696.

[9] Liu, R.; Fraylich, M.; Saunders, B. R., Thermoresponsive copolymers: from fundamental studies to applications. *Colloid and Polymer Science* 287, 6 (2009): 627-643.

[10] Hua, D.; Jiang, J.; Kuang, L.; Jiang, J.; Zheng, W.; Liang, H., Smart chitosan-based stimuli-responsive nanocarriers for the controlled delivery of hydrophobic pharmaceuticals. *Macromolecules* 44, 6 (2011): 1298-1302.

[11] dos Santos, J. E.; Dockal, E. R.; Cavalheiro, É. T. G., Synthesis and characterization of Schiff bases from chitosan and salicylaldehyde derivatives. *Carbohydrate Polymers* 60, 3 (2005): 277-282.

[12] Guinesi, L. S.; Cavalheiro, É. T. G., Influence of some reactional parameters on the substitution degree of biopolymeric Schiff bases prepared from chitosan and salicylaldehyde. *Carbohydrate Polymers* 65, 4 (2006): 557-561.

[13] Jin, X.; Wang, J.; Bai, J., Synthesis and antimicrobial activity of the Schiff base from chitosan and citral. *Carbohydrate Research* 344, 6 (2009): 825-829.

[14] Tree-udom, T.; Wanichwecharungruang, S. P.; Seemork, J.; Arayachukeat, S., Fragrant chitosan nanospheres: controlled release systems with physical and chemical barriers. *Carbohydrate Polymers* 86, 4 (2011): 1602-1609.

[15] Hann, R. M.; Jamieson, G. S.; Reid, E. E., Schiff Bases derived from 5-chlorovanillin. *Journal of the American Chemical Society* 51, 8 (1929): 2586-2588.

[16] Yao, Z.; Zhang, C.; Ping, Q.; Yu, L., A series of novel chitosan derivatives: synthesis, characterization and micellar solubilization of paclitaxel. *Carbohydrate Polymers* 68, 4 (2007): 781-792.

[17] Jeong, Y.-I.; Kim, D.-G.; Jang, M.-K.; Nah, J.-W., Preparation and spectroscopic characterization of methoxy poly(ethylene glycol)-grafted water-soluble chitosan. *Carbohydrate Research* 343, 2 (2008): 282-289.

[18] Choochottiros, C.; Yoksan, R.; Chirachanchai, S., Amphiphilic chitosan nanospheres: factors to control nanosphere formation and its consequent pH responsive performance. *Polymer* 50, 8 (2009): 1877-1886.

[19] Gumí, T.; Gascón, S.; Torras, C.; Garcia-Valls, R., Vanillin release from macrocapsules. *Desalination* 245, 1-3 (2009): 769-775.

[20] Sansukcharearnpon, A.; Wanichwecharungruang, S.; Leepipatpaiboon, N.; Kerdcharoen, T.; Arayachukeat, S., High loading fragrance encapsulation based on a polymer-blend: Preparation and release behavior. *International Journal of Pharmaceutics* 391, 1-2 (2010): 267-273.

[21] Aiping, Z.; Tian, C.; Lanhua, Y.; Hao, W.; Ping, L., Synthesis and characterization of N-succinyl-chitosan and its self-assembly of nanospheres. *Carbohydrate Polymers* 66, 2 (2006): 274-279.

[22] Opanasopit, P.; Ngawhirunpat, T.; Chaidedgumjorn, A.; Rojanarata, T.; Apirakaramwong, A.; Phongying, S.; Choochottiros, C.; Chirachanchai, S., Incorporation of camptothecin into N-phthaloyl chitosan-g-mPEG self-assembly micellar system. *European Journal of Pharmaceutics and Biopharmaceutics* 64, 3 (2006): 269-276.

[23] Opanasopit, P.; Ngawhirunpat, T.; Rojanarata, T.; Choochottiros, C.; Chirachanchai, S., N-Phthaloylchitosan-g-mPEG design for all-trans retinoic acid-loaded polymeric micelles. *European Journal of Pharmaceutical Sciences* 30, 5 (2007): 424-431.

[24] Anumansirikul, N.; Wittayasuporn, M.; Klinubol, P.; Tachaprutinun, A.; Wanichwecharungruang, S. P., UV-screening chitosan nanocontainers: Increasing the photostability of encapsulated materials and controlled release. *Nanotechnology* 19, 20 (2008): 1-9.

[25] Li, G.; Zhuang, Y.; Mu, Q.; Wang, M.; Fang, Y. e., Preparation, characterization and aggregation behavior of amphiphilic chitosan derivative having poly (l-lactic acid) side chains. *Carbohydrate Polymers* 72, 1 (2008): 60-66.

[26] Sui, W.; Wang, Y.; Dong, S.; Chen, Y., Preparation and properties of an amphiphilic derivative of succinyl-chitosan. *Colloids and Surfaces A: Physicochemical and Engineering Aspects* 316, 1-3 (2008): 171-175.

[27] Cai, G.; Jiang, H.; Chen, Z.; Tu, K.; Wang, L.; Zhu, K., Synthesis, characterization and self-assemble behavior of chitosan-O-poly(ε-caprolactone). *European Polymer Journal* 45, 6 (2009): 1674-1680.

[28] Gorochovceva, N.; Makuska, R., Synthesis and study of water-soluble chitosan-O-poly(ethylene glycol) graft copolymers. *European Polymer Journal* 40, 4 (2004): 685-691.

[29] Hu, Y.; Jiang, H.; Xu, C.; Wang, Y.; Zhu, K., Preparation and characterization of poly(ethylene glycol)-g-chitosan with water- and organosolubility. *Carbohydrate Polymers* 61, 4 (2005): 472-479.

[30] Casettari, L.; Vllasaliu, D.; Mantovani, G.; Howdle, S. M.; Stolnik, S.; Illum, L., Effect of PEGylation on the toxicity and permeability enhancement of chitosan. *Biomacromolecules* 11, 11 (2010): 2854-2865.

[31] Kong, X.; Li, X.; Wang, X.; Liu, T.; Gu, Y.; Guo, G.; Luo, F.; Zhao, X.; Wei, Y.; Qian, Z., Synthesis and characterization of a novel MPEG-chitosan diblock copolymer and self-assembly of nanoparticles. *Carbohydrate Polymers* 79, 1 (2010): 170-175.

[32] Hirano, S.; Hayashi, H., Some fragrant fibres and yarns based on chitosan. *Carbohydrate Polymers* 54, 2 (2003): 131-136.

[33] Wilhelm, M.; Zhao, C. L.; Wang, Y.; Xu, R.; Winnik, M. A.; Mura, J. L.; Riess, G.; Croucher, M. D., Poly(styrene-ethylene oxide) block copolymer micelle formation in water: a fluorescence probe study. *Macromolecules* 24, 5 (1991): 1033-1040.

[34] Chung, J. E.; Yokoyama, M.; Yamato, M.; Aoyagi, T.; Sakurai, Y.; Okano, T., Thermo-responsive drug delivery from polymeric micelles constructed using block copolymers of poly(N-isopropylacrylamide) and poly(butylmethacrylate). *Journal of Controlled Release* 62, 1-2 (1999): 115-127.

[35] Lutz, J.-F.; Akdemir, Ö.; Hoth, A., Point by point comparison of two thermosensitive polymers exhibiting a similar LCST: is the age of poly(NIPAM) Over?. *Journal of the American Chemical Society* 128, 40 (2006): 13046-13047.

[36] Nakayama, H.; Kaetsu, I.; Uchida, K.; Okuda, J.; Kitami, T.; Matsubara, Y., Preparation of temperature responsive fragrance release membranes by UV curing. *Radiation Physics and Chemistry* 67, 2 (2003): 131-136.

[37] Huang, X.; Du, F.; Cheng, J.; Dong, Y.; Liang, D.; Ji, S.; Lin, S.-S.; Li, Z., Acid-sensitive polymeric micelles based on thermoresponsive block copolymers with pendent cyclic orthoester groups. *Macromolecules* 42, 3 (2009): 783-790.

[38] Lage Robles, J.; Bochet, C. G., Photochemical release of aldehydes from α-acetoxy nitroveratryl ethers. *Organic Letters* 7, 16 (2005): 3545-3547.

[39] Dilip, M.; Griffin, S. T.; Spear, S. K.; Rodríguez, H. c.; Rijksen, C.; Rogers, R. D., Comparison of temperature effects on the salting out of poly(ethylene glycol) versus poly(ethylene oxide)−poly(propylene oxide) random copolymer. *Industrial & Engineering Chemistry Research* 49, 5 (2010): 2371-2379.

[40] Knop, K.; Hoogenboom, R.; Fischer, D.; Schubert, U. S., Poly(ethylene glycol) in drug delivery: pros and cons as well as potential alternatives. *Angewandte Chemie International Edition* 49, 36 (2010): 6288-6308.

[41] Tang, F.; Zhang, L.; Zhu, J.; Cheng, Z.; Zhu, X., Surface functionalization of chitosan nanospheres via surface-initiated AGET ATRP mediated by iron catalyst in the presence of limited amounts of air. *Industrial & Engineering Chemistry Research* 48, 13 (2009): 6216-6223.

APPENDIX

1. Determination of substitution degree of mPEG

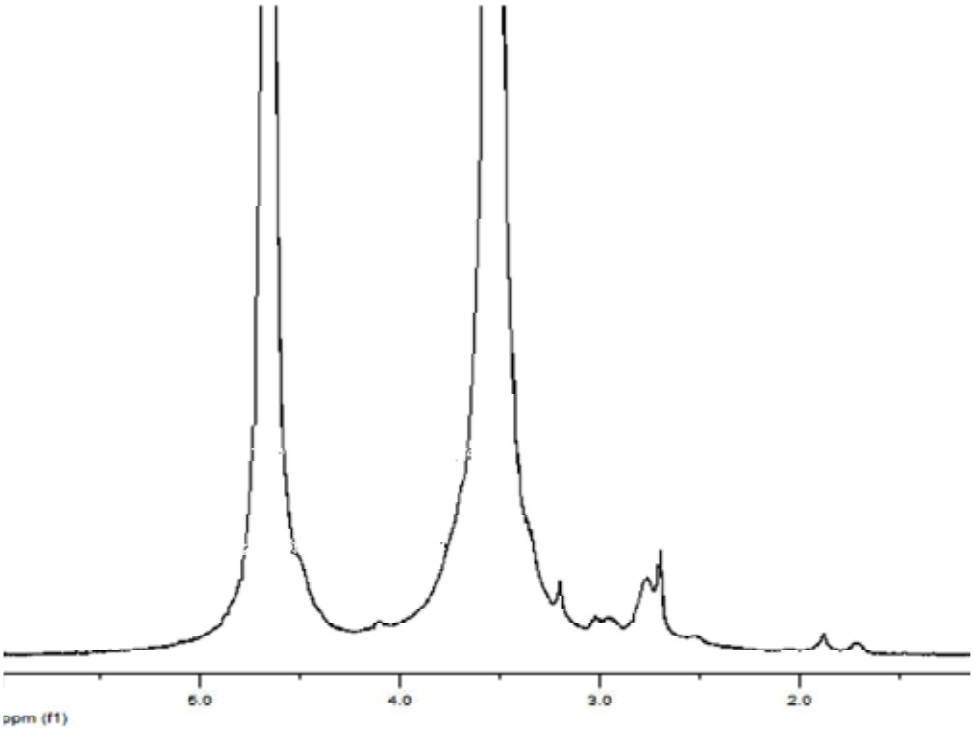

Figure A1. ^{1}H NMR spectrum of poly(ethylene oxide) grafted-chitosan (mPEO-CS)

The substitution degree of mPEG could be obtained by calculation using equation (1):

$$DG = \frac{I_{graft} \times DD}{n \times I_{CS}} \qquad (1)$$

I_{graft} = the intensity of grafted moiety

DD = deacetylation degree of chitosan

n = number of protons of grafted moiety

I_{CS} = the intensity of hydrogen atom of chitosan's glucosamine unit

According to ^{1}H NMR spectrum of mPEO-CS (Figure A1), the substitution degree of mPEG moiety could be calculated using integral ratio between 3 protons of mPEG moiety (δ 3.34 ppm) and 1 proton of C2 in glucosamine unit (δ 3.04 ppm) with 85% of deacetylation degree as followed:

$$DG = \frac{0.59 \times 0.85}{3 \times 1}$$

$$DG = 0.168$$

Therefore, the substitution degree of mPEG moiety which was calculated is equal to 0.168.

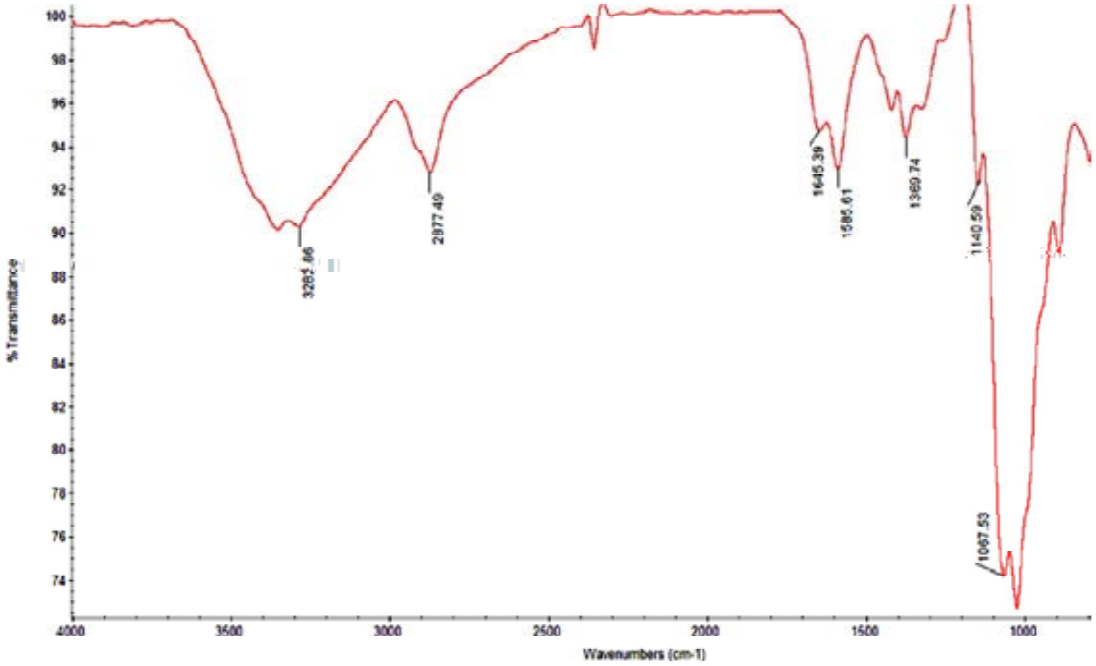

Figure A2. ATR-FTIR spectrum of chitosan

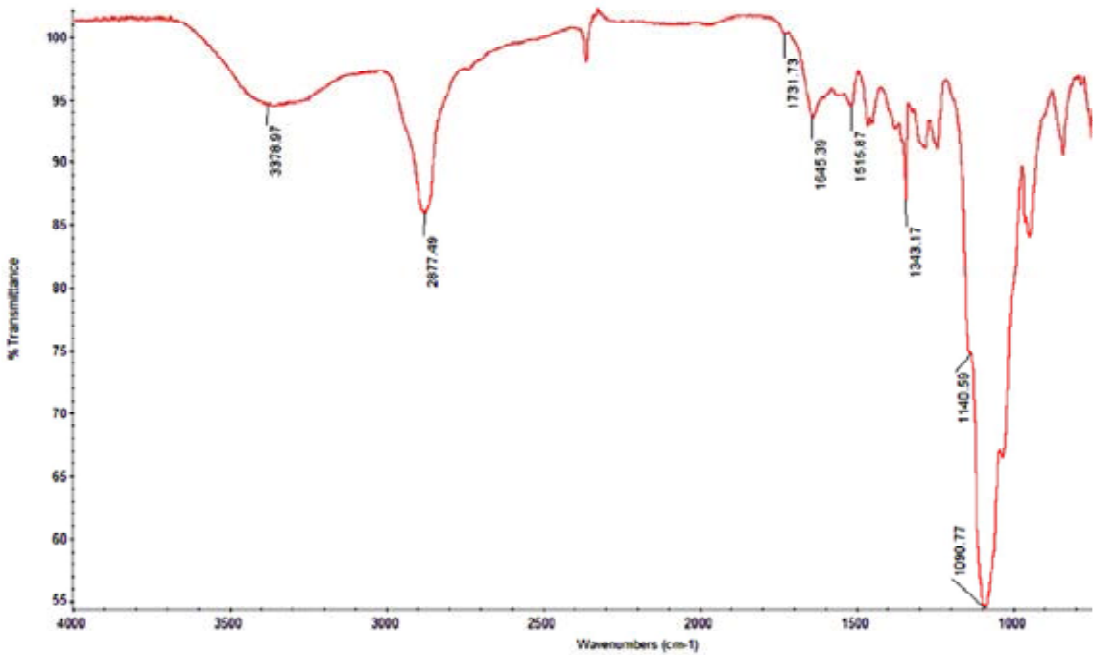

Figure A3. ATR-FTIR spectrum of poly(ethylene oxide) grafted-chitosan (mPEO-CS)

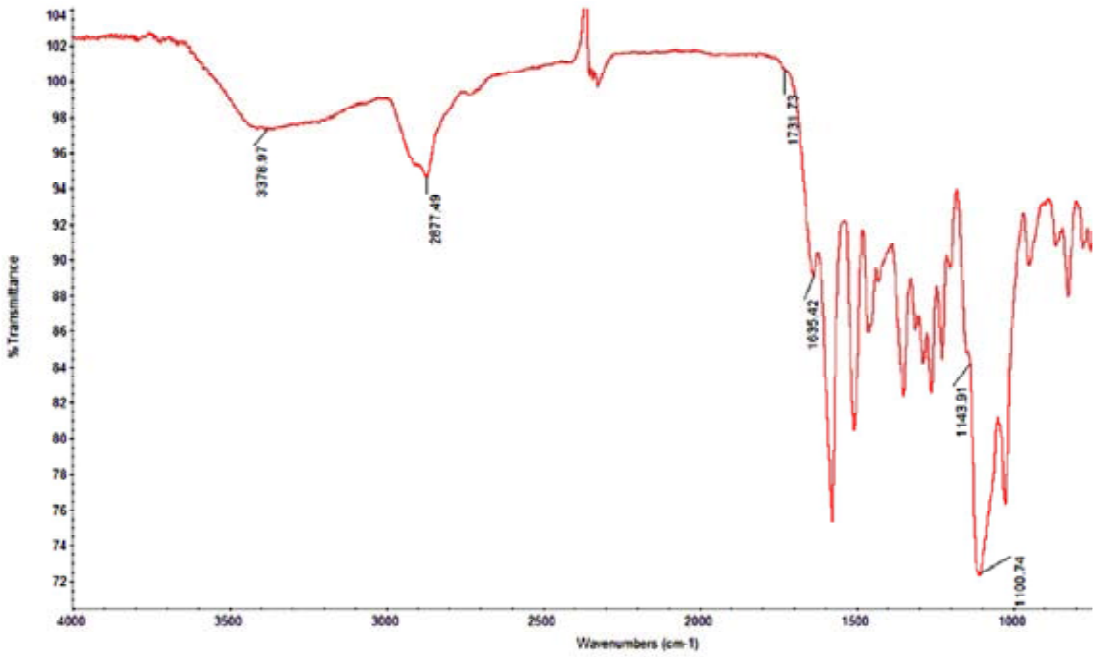

Figure A4. ATR-FTIR spectrum of vanillidene-mPEO-CS

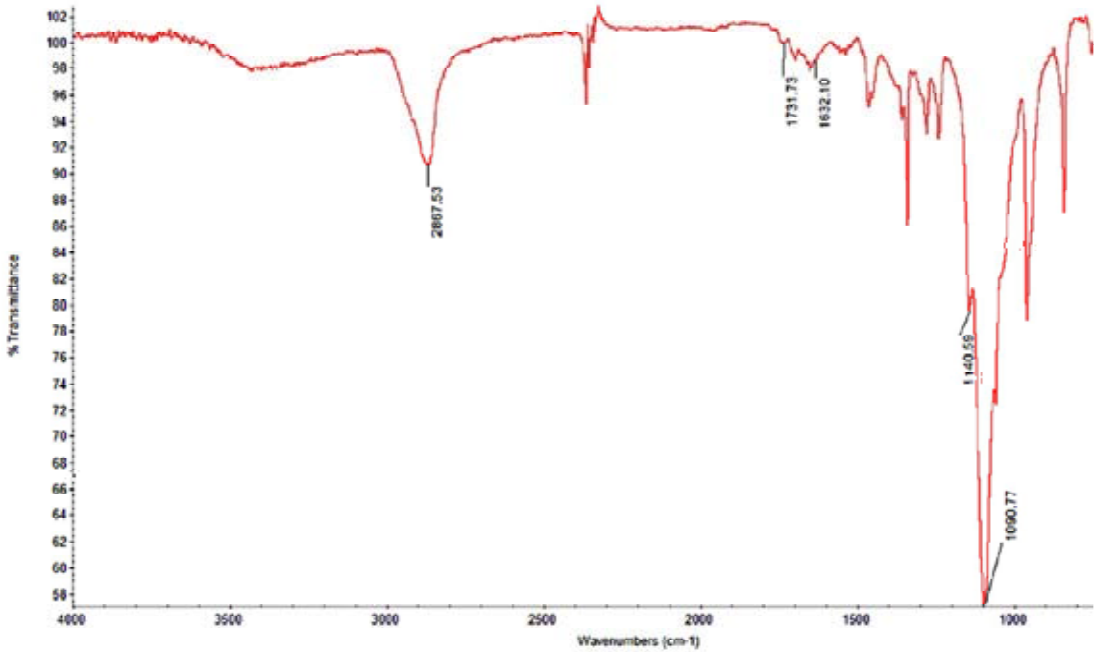

Figure A5. ATR-FTIR spectrum of citralidene-mPEO-CS

2. Evaluation of grafting degree of aldehydes

2.1 Grafting degree of vanillidene-mPEO-CS

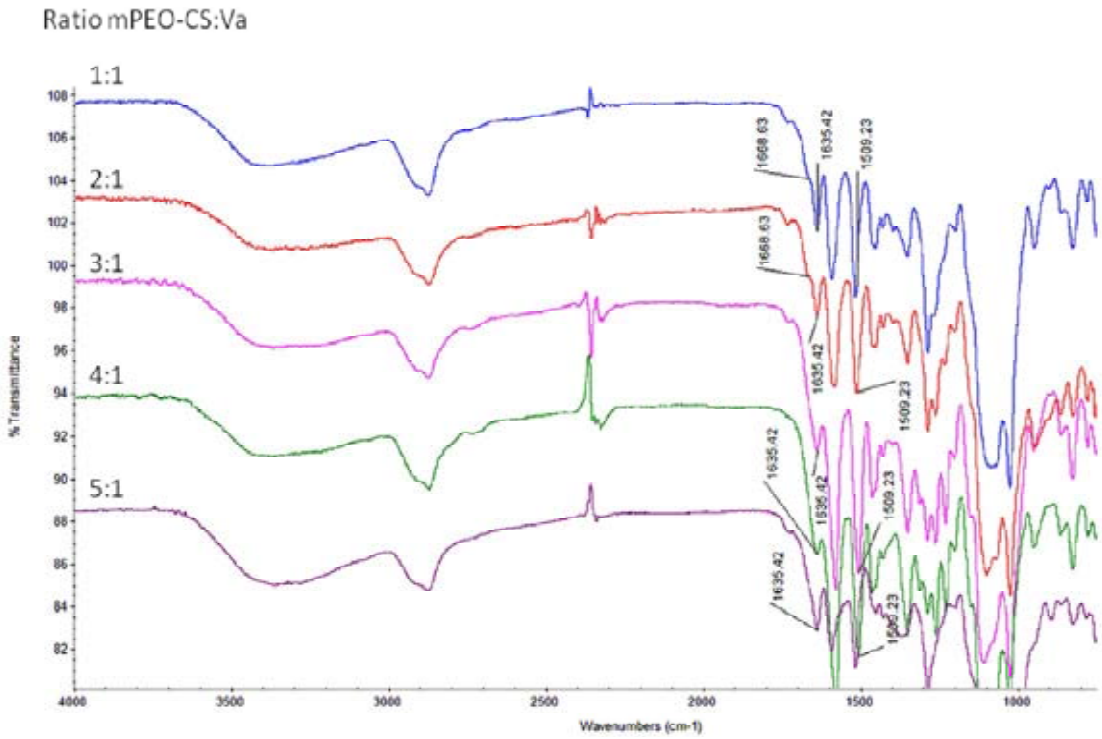

Figure A6. ATR-FTIR spectra of vanillidene-mPEO-CS with weight ratio of mPEO-CS to vanillin for 1:1, 2:1, 3:1, 4:1 and 5:1

An optimum weight ratio of mPEO-CS to perfumery aldehyde is the ratio with maximum grafted perfumery aldehyde and no free aldehyde left in the system. According to ATR-FTIR spectra of vanillidene-mPEO-CS, the ratio of mPEO-CS to vanillin for 3:1 is the ratio having the highest amount of grafted vanillin. It does not, moreover, show absorption peak around 1668 cm^{-1}, corresponding to C=O stretching vibration of free aromatic aldehyde.

2.2 Grafting degree of citralidene-mPEO-CS

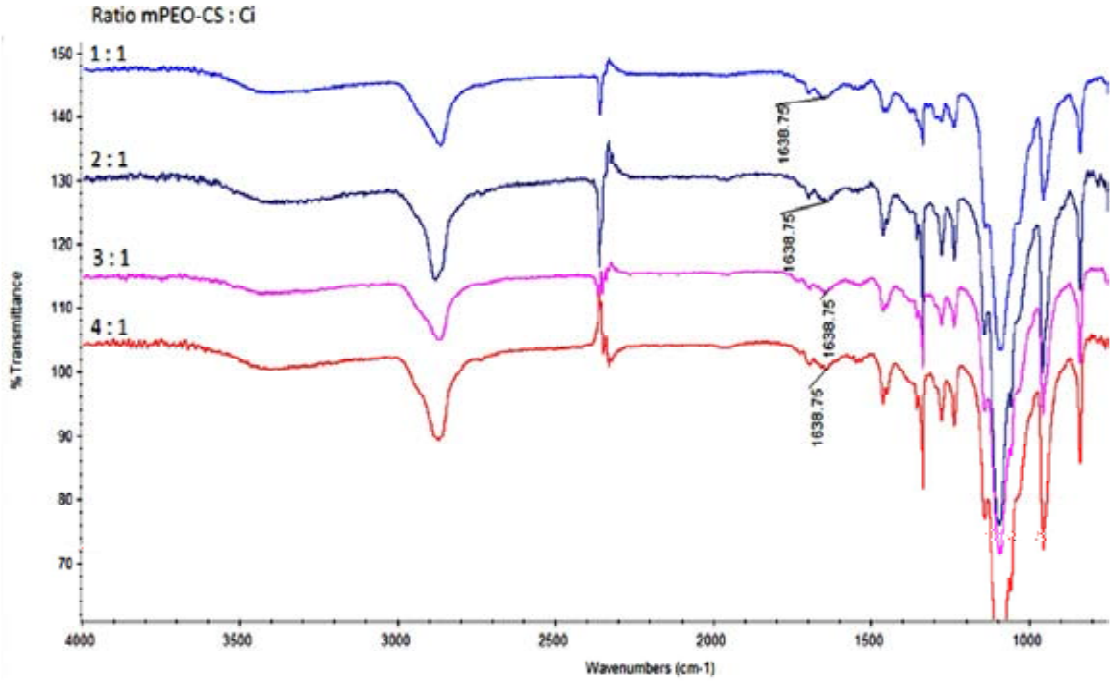

Figure A7. ATR-FTIR spectra of citralidene-mPEO-CS with weight ratio of mPEO-CS to citral for 1:1, 2:1, 3:1 and 4:1

According to ATR-FTIR spectra of citralidene-mPEO-CS, the ratio of mPEO-CS to citral for 3:1 is the ratio having the highest amount of grafted citral. In addition, It does not exhibit the absorption peak around 1668 cm^{-1}, corresponding to C=O stretching vibration of free aliphatic aldehyde.

.

Grafting degree of vanillin and citral

Mole of mPEO-CS

Weight of mPEO-CS 3000 ppm, 5 mL = 15 mg

Molecular weight of mPEO-CS (1 repeating unit) = 1024 g/mol

Thus, average molecular weight of 1 unit = 341.33 g/mol

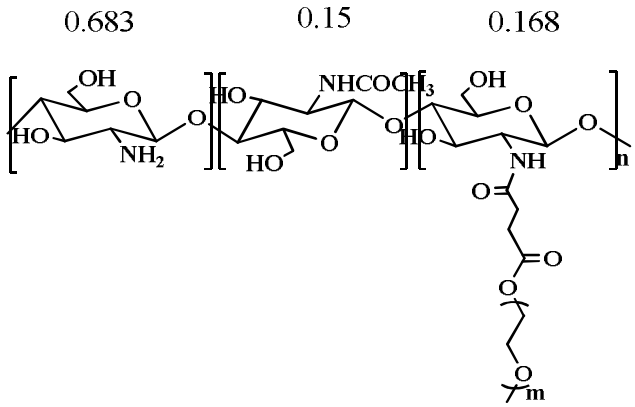

∴ Mole of mPEO-CS = 1.46×10^{-5} mol (per 3 units)

And per 1 unit, = 4.38×10^{-5} mol

Vanillin

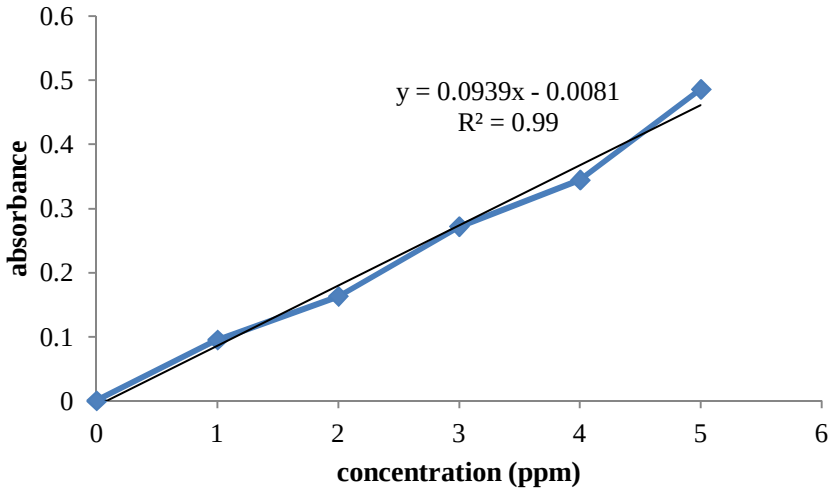

Figure A8. Calibration curve of various concentrations of vanillin in hexane at 269 nm

The amount of extracted vanillin was calculated based on Figure A8 using equation (2)

$$Y = 0.0939X - 0.0081 \quad (2)$$

$$0.6145 = 0.0939X - 0.0081$$

$$X = 6.6304$$

Dilution factor = 10

$$X = 6.6304 \times 10$$

$$X = 66.30 \text{ ppm}$$

Weight of grafted vanillin in 15 ml of hexane = 66.30 x 0.015

= 0.9946 mg

Molecular weight of vanillin = 152.15 g/mol

∴Mole of vanillin = 0.9946 mg/ 152.15 g/mol = 6.537×10^{-6} mol

DG of vanillin = $6.537 \times 10^{-6} / 4.38 \times 10^{-5} = 0.15$

Citral

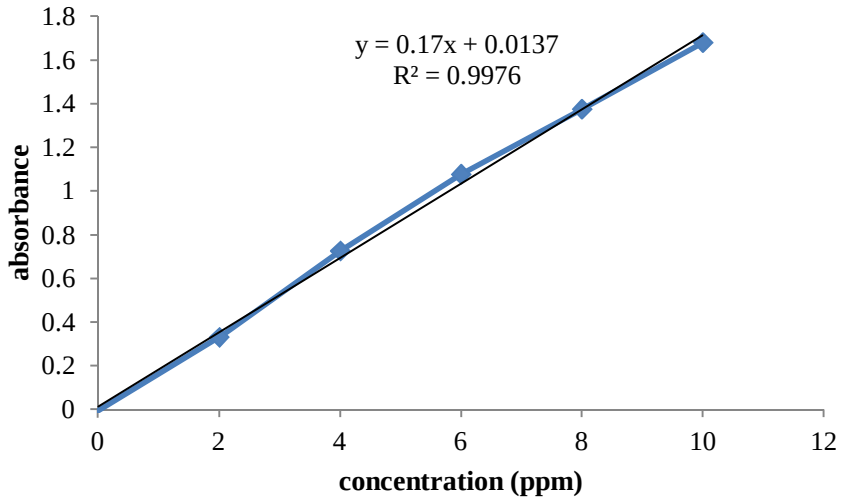

Figure A9. Calibration curve of various concentrations of citral in hexane at 242 nm

The amount of extracted citral was calculated based on Figure A9 using equation (3)

$$Y = 0.17X - 0.0137 \quad (3)$$

$$0.9535 = 0.17X - 0.0137$$

$$X = 5.5282$$

Dilution factor = 10

$$X = 5.5282 \times 10$$

$$X = 55.28 \text{ ppm}$$

Weight of grafted vanillin in 15 ml of hexane = 55.28 x 0.015

= 0.8292 mg

Molecular weight of vanillin = 152.24 g/mol

$\therefore$ Mole of vanillin = 0.8292 mg/ 152.24 g/mol = 5.447×10^{-6} mol

DG of vanillin = $5.447 \times 10^{-6} / 4.38 \times 10^{-5} = 0.12$

3. Calculation of released aldehydes

3.1 The amount of thermally released vanillin

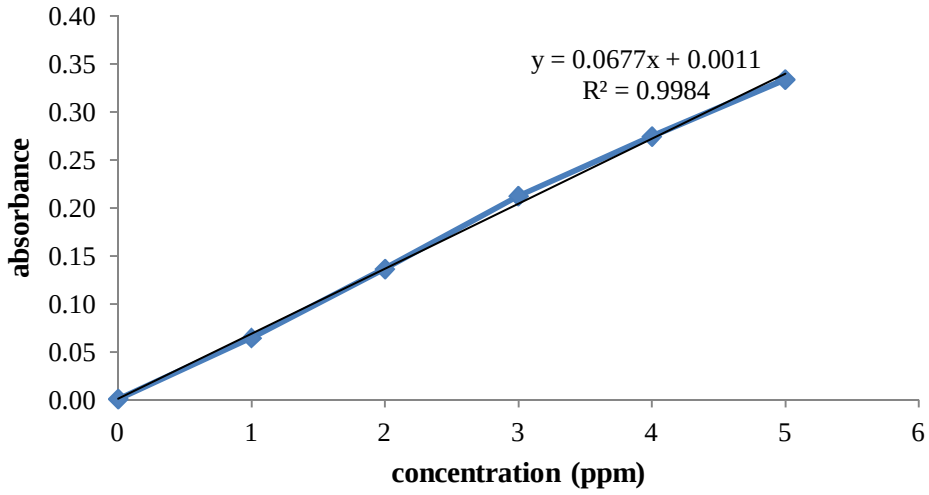

Figure A10. Calibration curve of various concentrations of vanillin in ethanol: H_2O (1:1) at 280 nm

The amount of remained vanillin at 0 day was calculated based on Figure A10 using equation (4)

$$Y = 0.0677X - 0.0011 \quad (4)$$

$$0.322 = 0.0677X - 0.0011$$

$$X = 4.74$$

Dilution factor = 33.33

$$X = 4.74 \times 33.33$$

$$X = 158 \text{ ppm}$$

Weight of grafted vanillin in 15 ml of ethanol: H_2O = 158 x 0.015

= 2.37 mg

Relative amount of remained vanillin at 0 day = (2.37/2.37) x 100

= 100%

∴Relative amount of released vanillin at 0 day = 100 -100 = 0%

The amount of remained vanillin at 10 day was calculated based on Figure A10 using equation (4)

$$Y = 0.0677X - 0.0011 \quad (4)$$

$$0.292 = 0.0677X - 0.0011$$

$$X = 4.30$$

Dilution factor = 33.33

$$X = 4.30 \times 33.33$$

$$X = 143.3 \text{ ppm}$$

Weight of grafted vanillin in 15 ml of ethanol: H_2O = 143.3 x 0.015

= 2.15 mg

Relative amount of remained vanillin at 0 day = (2.15/2.37) x 100

= 90.7%

∴Relative amount of released vanillin at 0 day = 100 -90.7 = 9.3%

3.2 The amount of thermally released citral

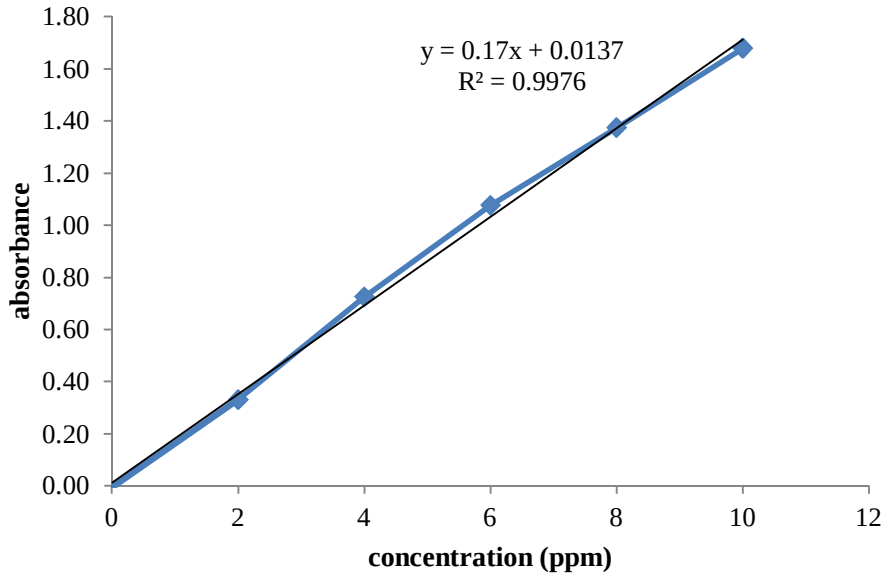

Figure A11. Calibration curve of various concentrations of citral in hexane at 242 nm

The amount of remained citral at 0 day was calculated based on Figure A11 using equation (3)

$$Y = 0.17X - 0.0137 \quad (3)$$

$$0.9535 = 0.17X - 0.0137$$

$$X = 5.5282$$

Dilution factor = 10

$$X = 5.5282 \times 10$$

$$X = 55.28 \text{ ppm}$$

Weight of grafted citral in 15 ml of hexane = 55.28 x 0.015

= 0.8292 mg

Relative amount of remained vanillin at 0 day = (0.8292/0.8292) x 100

= 100%

∴Relative amount of released vanillin at 0 day = 100 -100 = 0%

The amount of remained citral at 5 day was calculated based on Figure A11 using equation (3)

$$Y = 0.17X - 0.0137 \quad (3)$$

$$0.025 = 0.17X - 0.0137$$

$$X = 0.066$$

Dilution factor = 10

$$X = 0.066 \times 10$$

$$X = 0.665 \text{ ppm}$$

Weight of grafted citral in 15 ml of hexane = 0.665 x 0.015

= 0.010 mg

Relative amount of remained vanillin at 0 day = (0.010/0.8292) x 100

= 1.2%

∴Relative amount of released vanillin at 0 day = 100 -1.2 = 98.8%

VITAE

Miss Jiraporn Seemork was born on May 3, 1987 in Bangkok, Thailand. She received a Bachelor's Degree of Science in Chemistry from Kasetsart University in 2008. Then, she started her graduate study a Master's Degree in Program of Petrochemistry and Polymer Science, Faculty of Science, Chulalongkorn University. During her undergraduate study, she had received a scholarship from Human Resource Development in Science Project (Science Achievement Scholarship of Thailand, SAST) and during her master study, she had received a scholarship from National Center of excellence for Petroleum, Petrochemicals, and Advanced Materials (NCE-PPAM). She also had a great opportunity to present her work in the topic of "Fragrances-loaded temperature responsive copolymers for controlled release" in poster session at the 4th International Workshop on Polymer Engineering and Processing and 5th Seminar of the Research Center for Highly Environmental and Recyclable Polymer which were held at Japan Advanced Institute of Science and Technology, Japan.

Her present address is 422/740 Ratchavithi Rd., Tungphayathai, Ratchathewi, Bangkok Thailand 10400.